Dublin City University

School of Mathematical Sciences

M.Sc. Thesis

The Effect of Shear Flow on the Resistive Tearing Mode of Magnetohydrodynamics in a Cylindrical Geometry.

Néill Sweeney B.Sc.

Supervisors: Prof. A.D. Wood,
School of Mathematical Sciences.

Dr. Eugene O'Riordan,
School of Mathematical Sciences.

I hereby certify that this material which I now submit for assessment on the programme of study leading to the award of M.Sc. is entirely my own work and has not been taken from the work of others save to the extent that such work has been cited and acknowledged within the text of my work.

Signed: Néill Sweeney

Néill Sweeney

ID No. 96970847

Date 1 March, 1999

Acknowledgements:

I would like to acknowledge the assistance and direction provided by my supervisors Prof. Alastair Wood and Dr. Eugene O'Riordan. I would also like to acknowledge the assistance of Dr. Richard Paris in giving me a detailed set of workings to start from. This work was funded by Euratom.

M.Sc. Thesis Abstract

The Effect of Shear Flow on the Resistive Tearing Mode of Magnetohydrodynamics in a Cylindrical Geometry.

Néill Sweeney
7/Dec/1998

Resistive instabilities are unstable modes which disappear as resistivity tends to zero. Their growth time is proportional to a positive fractional power of resistivity. The equilibrium we consider has axial symmetry in a cylinder. With small but finite resistivity these modes originate about a surface, known as a resonant surface. Using the tearing ordering, we develop a system of ordinary differential equations to model the modes, including shear flow. We develop a numerical code to solve the system. We plot the loci of the growth time for increasing flow for a sample of the other parameters. We also plot marginal stability curves. Our results show a strong interaction between flow and some of the other parameters. We also include a couple of series solutions to the problem. One is valid as viscosity tends to infinity and the other as flow tends to infinity.

Introduction

The behaviour of confined high-temperature plasmas is complex and varied. An understanding of this behaviour is necessary for research into the possibility of generating power from nuclear fusion. It has been discovered that the magnetohydrodynamic (MHD) system describes a lot of the macroscopic behaviour of plasmas. This system considers the plasma as a conducting fluid in a magnetic field. It contains the Navier-Stokes equations as a subset. Even with this simplified model there is a wide range of possible behaviour.

In order to generate power the plasma must be heated while being confined by externally generated magnetic fields. Therefore initial theoretical research concentrated on finding stable equilibria. This appeared to be a depressing search. After much work many different categories of instability were identified but no stable equilibria. Experimental work, though, showed that the presence of an instability is not disastrous. More important is how the instability develops. In the early development of an instability, it will be small enough to be considered as a linear perturbation about the equilibrium being studied. It will grow exponentially with a fixed growth rate. Eventually non-linear terms will become significant. This occurs relatively early for MHD instabilities. Tracking the non-linear development of an instability involves much more work. Currently there is considerable work on numerically simulating this non-linear development. This is computationally intensive and requires powerful and sophisticated equipment.

Because of the quick transition to non-linear development, the value of the growth rate does not provide vital information. Faster linear growth rates do not always indicate faster non-linear development. Other information from the linear phase can be useful. Of course if there are no growing modes in the linear phase there will be no non-linear development.

As stated before, there are many categories of instabilities. We will concentrate on just one, the resistive tearing mode. The original paper on resistive instabilities is the 1963 paper of Furth, Killeen and Rosenbluth. Since then, there has been considerable work with a steady increase in the number of parameters included in the final system. We will consider six parameters. We will follow the orderings, approximations and transformations of previous work, checking that they are still appropriate when we add shear flow. Considering the complexity of the original system, these simplifications are amazingly successful in reducing to a fourth order system of ordinary differential equations. Because of this, the numerical work can be done on a standard PC.

In Chapter 1 we outline how the system we study is derived from the MHD system. We also compare this system with the equivalent system in previous work. This system is set on an infinite domain. In Chapter 2 we use asymptotics to estimate the behaviour at the ends of the domain. In Chapter 3 we describe the numerical methods we use to study this system. The approach we employ is quite specific to the peculiarities of the problem. In Chapter 4 we give series solutions as viscosity or shear flow tend to infinity. This chapter is independent of the flow of the work and is offered as an alternative approach. In Chapter 5 we present the results of our numerical work. In the Appendix we present in more detail the reduction of the full MHD system to the tearing mode system.

1. Physical Model

Our starting point is the MHD equations for an incompressible conducting fluid which are

The momentum equation

$$\rho\frac{dV}{dt} = -\nabla p + (\nabla \times B)\times B + \mu_{\perp}\nabla^2 V$$

The induction equation

$$\frac{\partial B}{\partial t} = \nabla \times (V \times B) + \eta\nabla^2 B$$

Mass conservation (1.1)

$$\frac{\partial \rho}{\partial t} + \nabla \cdot \rho \underline{V} = 0$$

The divergence condition

$$\nabla \cdot B = 0$$

Incompressible flow

$$\nabla \cdot V = 0$$

Here V and B are the velocity and magnetic fields,
ρ, p are the density and the pressure,
$\eta, \mu_{\perp}$ are the resistivity and the perpendicular viscocity.

We assume we have an equilibrium configuration (B_0, V_0, ρ_0, p_0). We are looking for a linear mode (B_1, V_1, ρ_1, p_1) about that equilibrium.

$$\rho_0\left(\frac{\partial V_1}{\partial t} + V_0 \cdot \nabla V_1 + V_1 \cdot \nabla V_0\right) + \rho_1(V_0 \cdot \nabla V_0)$$

$$= -\nabla p_1 - \nabla(B_0 \cdot B_1) + B_0 \cdot \nabla B_1 + B_1 \cdot \nabla B_0 + \mu_{\perp}\nabla^2 V_1$$

$$\frac{\partial B_1}{\partial t} = \nabla \times (V_0 \times B_1) + \nabla \times (V_1 \times B_0) + \eta\nabla^2 B_1 \qquad (1.2)$$

$$\frac{\partial \rho_1}{\partial t} + V_0 \cdot \nabla \rho_1 + V_1 \cdot \nabla \rho_0 = 0$$

$$\nabla \cdot B_1 = 0$$

$$\nabla \cdot V_1 = 0$$

We will confine ourselves to incompressible modes.

The equilibria we want to study have axial symmetry, i.e. in cylindrical co-ordinates

$$\begin{aligned} B_0 &= B_{0\theta}(r)e_\theta + B_{0z}(r)e_z \\ V_0 &= V_{0\theta}(r)e_\theta + V_{0z}(r)e_z \\ \rho_0 &= \rho_0(r) \end{aligned} \qquad (1.3)$$

where e_θ, e_z are the cylindrical basis vectors.

Since all equilibrium values are constant in the θ and z directions, the modes must vary like

$$f(r)\exp(im\theta + ikz + \omega t)\,. \qquad (1.4)$$

So instead of a system of partial differential equations, each wave number (combination of k and m) is studied separately by a system of ordinary differential equations. $Re(\omega)>0$ corresponds to an exponentially growing mode and $Re(\omega)<0$ corresponds to an exponentially decaying mode. If there are no growing modes the equilibrium is stable. The correct dimensionless number to consider the importance of resistivity is the inverse of the magnetic Reynolds number. Under fusion conditions this is usually small (typically of the order 10^{-3} to 10^{-7}) indicating that resistivity is a small parameter. Thus in a high temperature plasma we have the classic boundary layer scenario of a small parameter multiplying the highest derivative in an equation. Neglecting resistivity a second order differential equation for B_r can be formed. The coefficients of this equation depend on the equilibrium being studied. We will assume we have a solution to this equation. This equation may have a regular singular point at $r=r_s$ (defining what is known as the resonant or rational surface) where

$$F = \frac{m}{r}B_{0\theta} + kB_{0z} = 0 \qquad (1.5)$$

(NB the location of the boundary layer depends on the wave direction of the mode being considered at that time).

At r_s there may be a jump in B_r and/or in the derivative of B_r. of the particular mode under consideration. Close to r_s, and only close to r_s, will resistivity have to be considered Inside the layer, we need an ordering to eliminate insignificant terms. This is a good point to mention some of the orderings commonly used to study this type of problem. Ignoring resistivity a sufficiently strong driving force may induce an ideal interchange mode. This driving force is caused by a combination of an adverse pressure gradient and curvature in the equilibrium magnetic field. The stability condition for this mode is known as Suydam's criterion. If the driving force is too weak to drive an ideal mode it may drive a resistive interchange mode. The fast interchange mode corresponds to short wavelengths and is completely localised to the resonant surface. Because it has no effect on the main body of the plasma it is of little physical interest. Alternatively a slow interchange mode can be formed which has a slower growth time but is not localised.

If the driving force is of a smaller order than that required to drive an interchange mode, modes of a different character develop, known as tearing modes. These are the modes we will study. They are not localised. They exist in the absence of a driving force. There are two possible orderings. One is the strong viscous ordering in which viscosity dominates inertial terms and the other is the weak viscous ordering in which viscosity is comparable to inertial terms. When viscosity is made dimensionless in the strong viscous ordering it is typically of order 10^{-2}. This suggests the weak ordering is a better model and this is the one we use.

Modes	ideal inter-change	resistive fast inter-change	resistive slow inter-change	weak viscous resistive tearing	strong viscous resistive tearing
time scale	0	0	1/3	3/5	2/3
width of resistive layer	N/A	1/2	1/3	2/5	1/3
driving force	0	0	0	2/5	1/3

Table 0-1: The order of key quantities in different orderings in terms of powers of resistivity.

To do this the system (1.2) will be rescaled. To connect the solution in the surface with that outside for the tearing ordering we match the jump in the derivatives.

$$\Delta' = \lim_{r \to r_s +} \frac{B_r'}{B_r} - \lim_{r \to r_s -} \frac{B_r'}{B_r}. \qquad (1.6)$$

The reasons for this choice of matching parameter are given in previous work particularly Coppi et al. (1966) page 108.

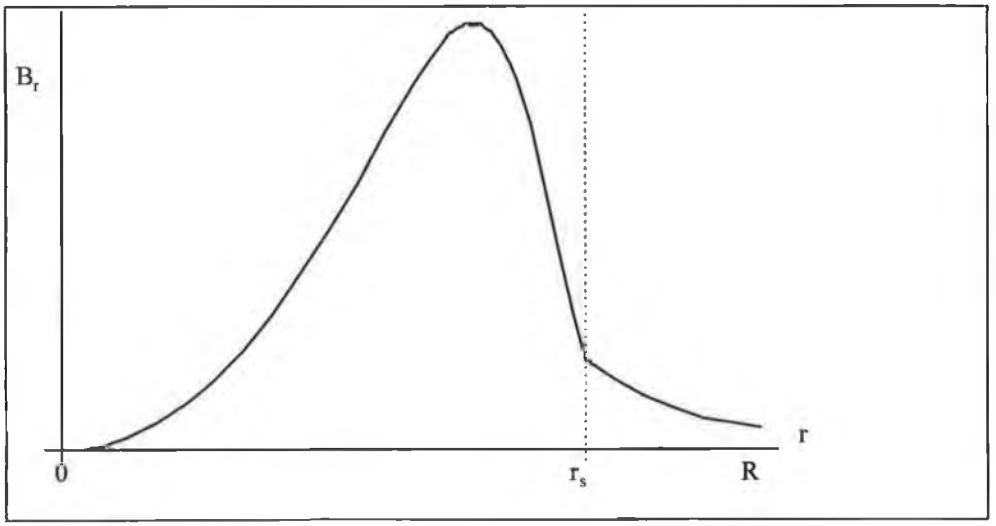

Figure 0-1: Typical B_r Profile for the tearing mode.;Biskamp (1993) p.67

Using this tearing ordering we eliminate insignificant terms inside the layer. The details here are quite involved and we leave them to the Appendix. (We are very grateful for a set of notes from Richard Paris on which that appendix is heavily dependent.). We then rescale variables and parameters relative to the length scale of the resistive layer and time scale of the mode. We employ the constant-Ψ approximation. For its range of validity see Furth et al. (1963) p464. We proceed to give the results of this scaling.

Scaled parameters for the weak viscous tearing ordering:

$$\text{length scale: } \delta = \left(\frac{\eta}{F'} \cdot \sqrt{\frac{\rho_0}{r_s}} \right)^{\frac{2}{5}} \qquad \text{time scale: } \tau = \frac{\eta}{\delta r_s}$$

$$X = \frac{r - r_s}{\delta} \qquad Q = \frac{\omega}{\tau} \qquad R = \frac{G'\delta}{\tau} \qquad \Gamma = \frac{\mu_\perp r_s}{\rho_0 \eta \delta} \qquad S = \frac{4kB_{0\theta}^2}{r_s^2 (F')^2}$$

(1.7)

$$D = -\frac{2p_0' k^2}{F'\delta} \qquad J_p = \frac{Ar_s}{\delta} \qquad \tilde{J} = -\frac{2kB_{0\theta}}{F'B_0} J_\parallel \ .$$

$$\left(\text{where } G = \tfrac{m}{r} V_{0\theta} + kV_{0z}\right)$$

The scaled versions of the variables are:

$$\Psi_0 = \frac{i}{F'\delta} B_{1r} \quad \Psi_1 = \frac{ir_s}{\delta^2 F'} B_{1r}^{(1)} \qquad \Xi = \frac{1}{\tau} V_{1r} \qquad Y = \frac{-2ik^2 B_0}{\delta (F')^2} B_\parallel$$

(1.8)

$$W = -\frac{2ik^2 B_0 \delta^2}{\eta} V_\parallel \ ,$$

and having eliminated insignificant terms we are left with the system:

$$\Psi_0'' = 0$$
$$\Psi_1'' = X\Xi + (Q + iRX)\Psi_0$$
$$\Gamma\Xi^{IV} + X^2\Xi - (Q + iRX)\Xi'' - Y = J_p\Psi_0 - (Q + iRX)X\Psi_0$$
$$Y'' + XW - S\Xi = 0$$
$$\Gamma W'' - (Q + iRX)W - XY = (D - \tilde{J}X)\Psi_0$$
(1.9)

(where the equations are respectively the induction equation in the radial direction to lowest order, the induction equation in the radial direction to next order, the momentum equation in the radial direction after the application of a differential operator, the induction equation parallel to the equilibrium magnetic field, the momentum equation parallel to equilibrium magnetic field.).

The jump in the derivative is

$$\Delta' = \frac{1}{\delta}\left(\lim_{X\to+\infty} \frac{\Psi'}{\Psi} - \lim_{X\to-\infty} \frac{\Psi'}{\Psi} \right).$$

Justification of the constant Ψ approximation

We outline heuristically the argument used to justify the constant-Ψ approximation. Full details and the range of validity are given in Furth et al. (1963) pp. 464. Because $\Psi_0''(x) = 0$, $\Psi_0(x)$ is a linear function. In the modes we consider $\frac{B_r'(r_s \pm)}{B_r(r_s \pm)}$ is finite, so $\frac{\Psi'(\pm\infty)}{\Psi(\pm\infty)}$ is small (because of the different length scales inside and outside the layer). Therefore to leading order Ψ is a constant. To normalise the modes, we take Ψ as 1 from here on. This makes the system inhomogeneous.

The matching condition then becomes.

$$\Delta' = \Psi_1'(+\infty) - \Psi_1'(-\infty) = \int_{-\infty}^{+\infty} \Psi_1'' dX = \int_{-\infty}^{+\infty} (X\Xi + (Q + iRX))dX.$$

The system then becomes

$$\boxed{\begin{aligned}&\Gamma\Xi^{IV} + X^2\Xi - (Q + iRX)\Xi'' - Y = J_p - (Q + iRX)X\\&Y'' + XW - S\Xi = 0\\&\Gamma W'' - (Q + iRX)W - XY = (D - \tilde{J}X)\\&\Delta' = \int_{-\infty}^{+\infty}(X\Xi + (Q + iRX))dX\end{aligned}}$$

(1.10)

The Effect of Shear Flow

What do we mean by the effect of shear flow? When we have motion parallel to a mode, we expect the frequency to be shifted (i.e. the Doppler-Shift). In our notation instead of ω, you get $(\omega + ik \cdot V_0)$ appearing in the equations. If we expand about the singular surface, r_s, we get

$$\omega + i(k \cdot V_0)(r) = \omega + i(k \cdot V_0)(r_s) + i(k \cdot V_0)'(r_s) \times (r - r_s)\ldots \qquad (1.11)$$

The constant term shifts the frequency of the mode but not the stability of the mode. It only shifts the imaginary part of the growth time. That is why we concentrate on the second term which when rewritten in terms of scaled parameters inside the layer becomes iRX. So Q (our scaled growth time) will be replaced by (Q+iRX). This destroys the symmetry of the equations about zero. We take flow small enough to allow us to neglect any other effect it may have. In particular, with the ordering we use here we can neglect the effects of Alfven waves, centrifugal forces and the Kelvin-Helmholtz instability.

Fourier Transform

We now use a Fourier transform on the system which reduces the order from eight to four.

Using the transforms

$$\xi(k) = \int_{-\infty}^{\infty} \Xi(X) e^{-ikX} dX \qquad \tilde{y}(k) = \int_{-\infty}^{\infty} Y(X) e^{-ikX} dX$$

$$w(k) = \int_{-\infty}^{\infty} W(X) e^{-ikX} dX \tag{1.12}$$

we transform each equation term by term.

Transforming (1.10a) we get

$$\Gamma k^4 \xi - \xi'' + Qk^2 \xi - R\left(k^2 \xi\right)' - \tilde{y} + 2\pi Qi\delta' - 2\pi Ri\delta'' = 2\pi J_p \delta . \tag{1.13a}$$

Transforming (1.10b) we get

$$-k^2 \tilde{y} + iw' - S\xi = 0 . \tag{1.13b}$$

Transforming (1.10c) we get

$$-\Gamma k^2 w - Qw + Rw' = i\tilde{y}' + 2\pi D\delta - 2\pi Ji\delta' . \tag{1.13c}$$

We remove the higher derivatives of the delta function by defining new variables.

$$\begin{aligned} h &= \xi + 2\pi Ri\delta \\ y &= \tilde{y} - 2\pi J\delta . \end{aligned} \tag{1.14}$$

So we get the system

$$\begin{aligned} &h'' + R(k^2 h)' - (Qk^2 + \Gamma k^4)h + y = -2\pi(J + J_p)\delta + 2\pi iQ\delta' \\ &iw' - k^2 y - Sh = -2\pi iSR\delta \\ &iy' + (Q + \Gamma k^2)w - Rw' = -2\pi D\delta \end{aligned} \tag{1.15}$$

The boundary conditions on this system are that all solutions have finite norm. The matching condition (1.10d), when transformed, becomes

$$\Delta' = \tfrac{i}{2}\left(h'(0-) + h'(0+)\right) \qquad (1.15d)$$

We need to impose some sensible boundary conditions on this system. The boundary conditions we will impose are that h, y and w have finite L_2 norm. This would be implied by $(\Xi - iR), \left(Y + \tilde{J}\right)$ and W having finite L_2 norm. As it can be derived from the ordering that these quantities are localised to the boundary layer these are reasonable boundary conditions.

If we replace the w′ in the third equation, using the second equation, we get

$$iy' + (Q + \Gamma k^2)w + R\left(ik^2 y + iSh\right) = -2\pi\left(D + SR^2\right)\delta. \qquad (1.16)$$

Thus we see that, the effective driving term is increased in the presence of flow. (S is by definition positive.) We will define the effective driving term as

$$D_R = D + SR^2. \qquad (1.17)$$

Comparison with previous work

This work is heavily dependent on work that went before. The aim is to study the effect of shear flow in a cylindrical geometry. We have two starting points. The first is recent work on the effect of shear flow on instabilities in slab geometry. In particular we are referring to papers by Paris and Sy (1983), Bondesson and Persson (1986), Paris et al. (1993)and Hou et al. (1996).The second is work on resistive instabilities in cylindrical geometry. In particular we refer to papers by Coppi et al. (1966) and Dagazian and Paris (1986). In order to compare this work with previous work, we write down the equivalent systems in those papers to the system we work with here (1.15). We changed notation and rearranged the equations where necessary to make the comparison.

Slab Geometry with Flow:

In the slab geometry the first equation of (1.15) decouples from the others. Because there is no natural driving term in the slab model, a gravitational field is included. The driving term, G, is then proportional to the equilibrium density gradient and the gravitational field. When S, D and G vanish the systems are identical.

$$\boxed{\begin{aligned} &h'' + R(k^2 h)' - \left(Qk^2 + \Gamma k^4\right)h + Gu = Q\delta' - iJ\delta \\ &Ru' = Qu - h + iR\delta \end{aligned}} \qquad (1.18)$$

where u is an artificial variable defined to facilitate the comparison.

Cylindrical Geometry without Flow:

Coppi, Greene and Johnson (1966):

Coppi, Greene and Johnson worked in cylindrical geometry. They did not include viscosity or flow, which we do. They did however include compressibility terms, which we do not.

$$\boxed{\begin{aligned} &h'' - Qk^2 h + y = Q\delta' \\ &iw' - k^2 y - (S - cD)h - cQy = 0 \\ &iy' + Qw = D\delta \end{aligned}}$$

($\beta = \frac{2p_0(r_s)}{B_0^2(r_s)}$ and γ is the adiabatic constant)

(1.19)

where c represents the compressibility term. $c = \frac{2}{\gamma\beta} \times \frac{\delta}{r_s}$.

Dagazian and Paris (1986):

Dagazian and Paris also work in a cylindrical geometry. They do include viscosity, parallel viscosity and compressibility terms, but not flow. Because they were looking for stationary modes, they set Q=0.

$$\boxed{\begin{aligned} &h'' - (\tfrac{1}{2}\Lambda((S - cD) + \Gamma k^4)h + y + \Lambda w' = 0 \\ &iw' - k^2 y - (S - cD)h = 0 \\ &iy' - \Gamma k^2 w + 2\Lambda(w'' - \tfrac{1}{2}(S - cD)h') = D\delta \end{aligned}}$$

Λ is the parallel viscosity

(1.20)

Only the odd part of the solution contributes to the matching parameter. Without the flow term, the systems of equations are symmetric. The current term, J, is even and therefore cannot affect the odd part of the solution. Therefore when R=0, the current does not affect the growth time and in papers without flow it is ignored.

Bondesson, Iacono and Bhatarjee (1987):

This paper is concerned with the effect of shear flow on ideal interchange modes in a cylindrical geometry. On page 2169 of their paper they give a complicated formula (8b) for the effective driving term in the presence of flow. Because the flows we consider are on a smaller scale than those considered in their paper, that formula can be considerably simplified. In

the ordering and notation of this work, that formula becomes ($D+SR^2$), which provides confirmation for our result.

Discussion: Compressibility

We completely neglect compressibility. As explained in Coppi et al. (1966) this is not correct even though the velocity field is to leading order divergence free. Quoting directly

> .... The divergence of the fluid velocity must nearly vanish. ...This does not mean that the divergence of the fluid velocity must play no role in the final results, but only that the dominant part of the velocity field must be divergence-free.

There are two reasons for our neglect of compressibility. Firstly we need to limit the number of parameters in the problem. Secondly, according to Coppi et al. (1966), the differences between the D-mode in the cylinder and G-mode in the slab are most pronounced in the limit in which the fluid is incompressible. Again quoting directly

> In most cases the effect of gravity and line curvature are interchangeable but in this case there are interesting differences. When gravity is the destabilising agent the driving force in the annihilated momentum equation, corresponding to eq. 50 (our eq.1), is proportional to the perturbed density and directly related to the fluid displacement. This is because gravity acts directly on the fluid. On the other hand, line curvature acts through the tension in the magnetic field lines and the corresponding driving terms are proportional to the component of the perturbed magnetic field parallel to the equilibrium field or, through eq32[$\frac{1}{2}B_1^2 + p_1 \approx 0$], to the perturbed pressure.
>
> Frequently the perturbed pressure and perturbed density are simply proportional and the two destabilising forces are similar, but they lead to quite different results in the limit in which the fluid is incompressible. .....

This can also be seen by comparing the terms in Coppi et al. (1966) proportional to c in (1.19) and the second equation in the slab (1.18).

2. Asymptotics

Behaviour at Infinity

The system has an irregular singular point as k tends to infinity. To estimate the behaviour at infinity, we use a dominant balance argument. Firstly we combine all three equations into one fourth order differential equation in h.

$$\begin{aligned}&\left(\Gamma k^2+Q\right)h^{IV}+\left(2\Gamma Rk^4+2QRk^2-2\Gamma k\right)h'''+\\&\left(\left(\Gamma R^2-2\Gamma^2\right)k^6+\left(QR^2-4\Gamma Q\right)k^4+4\Gamma Rk^3-2Q^2k^2+8QRk\right)h''+\\&\left(\begin{array}{l}-2\Gamma^2Rk^8-\Gamma QRk^6+\left(4\Gamma R^2-6\Gamma^2\right)k^5-2Q^2Rk^4+\left(6QR^2-10\Gamma Q\right)k^3+\\(-\Gamma RS-2\Gamma R)k^2-4Q^2k+(6QR-QRS)\end{array}\right)h'+\\&\left(\begin{array}{l}\Gamma^3k^{10}+3\Gamma Q^2k^8-6\Gamma^2k^7+3\Gamma Q^2k^6-12\Gamma QRk^5+\left(Q^3+S\Gamma^2+2\Gamma R^2-4\Gamma^2\right)k^4\\-6Q^2Rk^3+\left(6QR^2+2S\Gamma Q-10\Gamma Q\right)k^2+(2S\Gamma R-4\Gamma R)k+\left(SQ^2-2Q^2\right)\end{array}\right)h=0\end{aligned}$$

(2.1)

(We neglect the inhomogeneous terms as these are concentrated about zero.) We then assume the behaviour of h at infinity is of the form $h(k)\sim e^{a\frac{k^n}{n}}$. Substituting this form into the fourth order differential equation, we form a dominant balance equation consisting of terms proportional to k^{mn+c}, where m is 0,1,2,3,4. For every m, we pick out the term with maximum c as these are the only terms that could dominate at infinity.

$$\Gamma a^4k^{4n+2}\ldots+2RTa^3k^{3n+5}\ldots+\left(R^2-2\Gamma\right)\Gamma a^2k^{2n+8}\ldots-2\Gamma^2Rak^{n+11}\ldots+\Gamma^3k^{14}\ldots=0$$

(2.2)

The only possible balance is at n=3. This yields a fourth order polynomial equation for a. This equation can be factorised to yield:

$$\left(a^2+Ra-\Gamma\right)^2=0.\qquad(2.3)$$

We then get two double roots.

$$a = \frac{-R \pm \sqrt{4\Gamma + R^2}}{2} \tag{2.4}$$

Therefore two of the solutions grow exponentially and two decay at either endpoint. As all solutions must have finite norm this provides two boundary conditions at each end (i.e. the correct number of boundary conditions).

A similar procedure can be used to extend the approximation to the next order. This time we take h to be of the form $h(k) \sim e^{a\frac{k^3}{3}+a_1\frac{k^{n_1}}{n_1}}$. We found $n_1=1$ and $a_1 = \frac{Q}{\sqrt{4\Gamma + R^2}}$. We could continue to generate a full asymptotic series but we decide to stop here, as the accuracy is sufficient for the numerics.

We do not consider the case when both Γ and R tend to zero.

We can now set natural boundary conditions for the numerical work.. The equations are set on an infinite domain but numerically we work on a finite domain $[-L, L]$. The boundary conditions we impose are then

$$h'(-L) - \left(\left(\frac{-R + \sqrt{4\Gamma + R^2}}{2}\right)L^2 + \frac{Q}{\sqrt{4\Gamma + R^2}}\right)h(-L) = 0 \tag{2.5a}$$

and

$$h'(L) - \left(\left(\frac{-R - \sqrt{4\Gamma + R^2}}{2}\right)L^2 + \frac{Q}{\sqrt{4\Gamma + R^2}}\right)h(L) = 0 \tag{2.5b}$$

and similarly for y . This means the numerical solutions connect onto the correct asymptotic solutions at the endpoints.

Typically there is only a small improvement in accuracy using this approach from the standard approach of setting the solutions to zero at each end point. The exception is when $Re(Q)<0$ and Γ is small. Here we will have $a<<a_1$ at the left end of the range and the k^3 term will not dominate until relatively large k. With $Re(Q)<0$, a_1 is negative and the solution will grow until this happens. Using these boundary conditions the numerical solution will patch onto the correct behaviour at a reasonable choice of finite endpoint even though the solution is still growing at that point.

3. Numerical Methods

The problem we want to solve is

Given the parameters $\Delta', D, \Gamma, S, J, R \in \mathbb{R}$

Find all growth rates $Q \in \mathbb{C}$ and modes

$$(h(k) \quad y(k) \quad w(k)) \qquad \forall k \in (-\infty, \infty)$$

such that

$$\begin{aligned} &h'' + R(k^2 h)' - (Qk^2 + \Gamma k^4)h + y = -2\pi J\delta + 2\pi i Q\delta' \\ &iw' - k^2 y - Sh = -2\pi i SR\delta \\ &iy' + (Q + \Gamma k^2)w - Rw' = -2\pi D\delta \end{aligned} \tag{3.1}$$

and h, y and w have finite L_2 norm

and

$$\tfrac{i}{2}\left(h'(0-) + h'(0+)\right) = \Delta' \tag{3.1d}$$

Specifically we are interested in the mode with the growth rate, Q, which has the largest real part. This is the fastest growing mode which will eventually dominate the others.

Instead of approaching the problem directly we form a complex function.

Definition: $\Delta(Q,D,\Gamma,S,J,R)=\frac{i}{2}(h'(0-)+h'(0+))$

where $\begin{pmatrix} h & y & w \end{pmatrix}$ is the mode such that

$$\begin{aligned} &h''+R(k^2h)'-(Qk^2+\Gamma k^4)h+y=-2\pi J\delta+2\pi iQ\delta' \\ &iw'-k^2y-Sh=-2\pi iSR\delta \\ &iy'+(Q+\Gamma k^2)w-Rw'=-2\pi D\delta \end{aligned} \qquad (3.2)$$

and h, y and w have finite L_2 norm.

Solving the original problem is now a question of finding the Q-roots of

$$\Delta(Q,\cdots)-\Delta'=0. \qquad (3.3)$$

This is a good point at which to state some symmetrical properties of the problem given in Hou (1994) pp. 38 and still valid for this system.

$$\begin{aligned} &\Delta(Q,D,\Gamma,S,-J,R)=\bar{\Delta}(Q,D,\Gamma,S,J,R) \\ &\Delta(Q,D,\Gamma,S,J,-R)=\bar{\Delta}(Q,D,\Gamma,S,J,R). \end{aligned} \qquad (3.4)$$

$\bar{a}$ is the complex conjugate of a

Because of these properties, we only consider $R\geq 0$ and $J\geq 0$. In papers that do not include flow it is shown that J can have no effect on stability i.e.

$$\Delta(Q,D,\Gamma,S,J,0)=\Delta(Q,D,\Gamma,S,0,0). \qquad (3.5)$$

Whether a set of parameters (Δ',D,Γ,J,S,R) allows an unstable mode (i.e. one for which Re(Q)>0) is of more interest than the value of the growth rate, Q. Holding the other parameters fixed, there is a critical value of Δ' which we call Δ_0. For values of Δ' greater than Δ_0 there is at least one unstable mode. To identify this critical value, we will again work with the function we have just defined. At this critical value a mode will be moving from the stable (left) half of complex Q-plane to the unstable (right) half of the complex Q-plane via Re(Q)=0. Δ' is real so we look along the

imaginary Q-axis for points at which Im(Δ(Q,....))=0. Of these points the one with the least Re(Δ(Q,...)) is Δ_0. Writing concisely

Definition:

$$\Delta_0(D,\Gamma,S,J,R) = \min\{\Delta(Q,D,\Gamma,S,J,R) \quad |\Delta, iQ \in \Re \tag{3.6}$$

Approximation of Δ(Q,....)

The system consists of a second order and two first order equations. For convenience we put the two first order equations together. The mechanics were performed using Mathematica®. The equations then become:

$$\begin{aligned}
&h'' + R\left(k^2 h\right)' - \left(Qk^2 + \Gamma k^4\right)h + y = 2\pi J\delta + 2\pi i Q\delta' \\
&\left(Q + \Gamma k^2\right)y'' + \left(-2\Gamma k + QRk^2 + \Gamma Rk^4\right)y' + \\
&\left(2QRk - Q^2k^2 - 2\Gamma Qk^4 - \Gamma^2 k^6\right)y + \\
&S\begin{pmatrix}\left(QR + \Gamma Rk^2\right)h' + \\ \left(-Q^2 - 2\Gamma Rk - 2\Gamma Qk^2 - \Gamma^2 k^4\right)h\end{pmatrix} = -2\pi i Q^2 RS\delta + 2\pi i Q\left(D + SR^2\right)\delta'
\end{aligned} \tag{3.7}$$

(Notice that the second equation appears to have a regular singular point at k=0 when Q=0. Also notice that the right hand side disappears when Q=0. So this approach will have difficulties at the point Q=0)

This gives a system of two second order equations in two variables with 4 boundary conditions. These boundary conditions will be specified later. This system was solved by a standard finite element method on a finite range.

A weak form of this system is:

Find $h, y \in L_2$ such that

$$-(h', v') + R\left((k^2 h)', v\right) - Q(k^2 h, v) - \Gamma(k^4 h, v) + (y, v) = 2\pi J(\delta, v) + 2\pi i Q(\delta', v)$$

$$-Q(y', v') - \Gamma(k^2 y', v') - 4\Gamma(k y', v) + QR(k^2 y', v) + \Gamma R(k^4 y', v) + 2QR(ky, v)$$
$$-Q^2(k^2 y, v) - 2\Gamma Q(k^4 y, v) - \Gamma^2(k^6 y, v) +$$
$$S\left(QR(h', v) + \Gamma R(k^2 h', v) - Q^2(h, v) - 2\Gamma R(kh, v) - 2\Gamma Q(k^2 h, v) - \Gamma^2(k^4 h, v)\right) =$$
$$-2\pi i Q^2 RS(\delta, v) + 2\pi i Q\left(D + SR^2\right)(\delta', v)$$

$\forall v \in L_2$

where $(h, v) = \int_{-\infty}^{\infty} h\bar{v}dk$

(3.8)

We use hat functions as basis functions, defined by

$$b_j = \begin{cases} 0 & k < (j-1)s \\ \frac{k}{s} + (1-j) & (j-1)s < k < js \\ -\frac{k}{s} + (1+j) & js < k < (j+1)s \\ 0 & (j+1)s < k \end{cases}$$ (where s is the spacing of the nodes.)

(3.10)

We then write

$\tilde{h} = \sum_{j=-n+\frac{1}{2}}^{n-\frac{1}{2}} h_j b_j \quad \tilde{y} = \sum_{j=-n+\frac{1}{2}}^{n-\frac{1}{2}} h_j b_j$ which have finite support $[-L, L]$ where $L = (n + \frac{1}{2})s$.

Now that we are working on a finite support we need boundary conditions which correspond to h and y having finite L_2 norm. The conditions we will impose are that the finite element approximations patch onto the asymptotic approximations from the previous chapter.

Defining

$$\alpha_- = \left(\frac{-R+\sqrt{4\Gamma+R^2}}{2}\right)L^2 + \frac{Q}{\sqrt{4\Gamma+R^2}}$$

$$\alpha_+ = \left(\frac{-R-\sqrt{4\Gamma+R^2}}{2}\right)L^2 + \frac{Q}{\sqrt{4\Gamma+R^2}}$$

The boundary conditions are

$$\frac{\tilde{h}'(-L)}{\tilde{h}(-L)} = \alpha_- \quad \frac{\tilde{y}'(-L)}{\tilde{y}(-L)} = \alpha_- \quad \frac{\tilde{h}'(L)}{\tilde{h}(L)} = \alpha_+ \quad \frac{\tilde{y}'(L)}{\tilde{y}(L)} = \alpha_+$$

(3.11a)

The finite element approach then consists of

Find $\tilde{h}, \tilde{y}$ such that

$$-\left(\tilde{h}', b_i'\right) + R\left(\left(k^2\tilde{h}\right)', b_i\right) - Q\left(k^2\tilde{h}, b_i\right) - \Gamma\left(k^4\tilde{h}, b_i\right) + \left(\tilde{y}, b_i\right) =$$

$$2\pi J\left(\delta, b_i\right) + 2\pi i Q\left(\delta', b_i\right)$$

$$-Q\left(\tilde{y}', b_i'\right) - \Gamma\left(k^2\tilde{y}', b_i'\right) - 4\Gamma\left(k\tilde{y}', b_i\right) + QR\left(k^2\tilde{y}', b_i\right) + \Gamma R\left(k^4\tilde{y}', b_i\right) +$$

$$2QR\left(k\tilde{y}, b_i\right) - Q^2\left(k^2\tilde{y}, b_i\right) - 2\Gamma Q\left(k^4\tilde{y}, b_i\right) - \Gamma^2\left(k^6\tilde{y}, b_i\right) +$$

$$S\left(QR\left(\tilde{h}', b_i\right) + \Gamma R\left(k^2\tilde{h}', b_i\right) - Q^2\left(\tilde{h}, b_i\right) - 2\Gamma R\left(k\tilde{h}, b_i\right) - 2\Gamma Q\left(k^2\tilde{h}, b_i\right) - \Gamma^2\left(k^4\tilde{h}, b_i\right)\right) =$$

$$-2\pi i Q^2 RS\left(\delta, b_i\right) + 2\pi i Q\left(D + SR^2\right)\left(\delta', b_i\right)$$

$$\forall b_i \quad | i \in \left\{-n+\tfrac{3}{2}, -n+\tfrac{5}{2}, \cdots, n-\tfrac{5}{2}, n-\tfrac{3}{2}\right\}$$

and $\tilde{h}, \tilde{y}$ satisfy the boundary conditions described above (3.12)

All the coefficients are polynomials so the necessary integration can be done symbolically. The delta functions are dealt with in a natural way i.e.

$$\left(\delta, b_{-\frac{1}{2}}\right) = \tfrac{1}{2} \qquad \left(\delta, b_{\frac{1}{2}}\right) = \tfrac{1}{2}$$

$$\left(\delta', b_{-\frac{1}{2}}\right) = \tfrac{1}{2}s \qquad \left(\delta', b_{\frac{1}{2}}\right) = -\tfrac{1}{2}s \qquad (3.13)$$

We arrange the resulting system of equations into a matrix with bandwidth of 7. Having solved this linear system by Gaussian elimination, the matching parameter can then be estimated

$$\tilde{\Delta} = \frac{1}{s} i\left(h_{-\frac{1}{2}} - h_{-\frac{3}{2}} + h_{\frac{3}{2}} - h_{\frac{1}{2}} \right). \tag{3.14}$$

From now on we now drop the tildes from the approximations.

Verification of the Numerics

To check the numerics and to estimate the errors involved we ran some numerical experiments. The first was to increase, **n**, the number of elements keeping L, the end point, fixed. We give four examples fixing L at 2.5.

	Q=1 D=.5 Γ=.25 S=.1 J=2 R=1	Q=i D=1 Γ=1 S=.5 J=0 R=0	Q=-0.5+0.5i D=1 Γ=.025 S=1 J=.5 R=.1	Q=-.75 D=-1 Γ=1 S=0 J=0 R=3
n	Δ	Δ	Δ	Δ
16	1.3183+1.1219i	-1.7297+2.8434i	-1.6663+0.4921i	3.8403
32	1.2053+1.2480i	-1.9076+2.8730i	-1.7003+0.4874i	5.1753
64	1.1534+1.2826i	-1.9979+2.8807i	-1.7178+0.4857i	6.1267
128	1.1289+1.2916i	-2.0434+2.8827i	-1.7267+0.4850i	6.3939
256	1.1170+1.2939i	-2.0663+2.8832i	-1.7311+0.4847i	6.4670
512	1.1111+1.2945i	-2.0778+2.8833i	-1.7333+.04845i	6.4857

Table 3-1: Four examples of Δ calculated with an increasing number of elements, a fixed endpoint of L=2.5 and the asymptotic boundary conditions.

We can see that the results appear to be converging as n increases.

We also check the error due to curtailing the range. To do this we hold the spacing, s, fixed at .01 and vary the endpoint. For the same four examples

	Q=1 D=.5 Γ=.25 S=.1 J=2 R=1	Q=i D=1 Γ=1 S=.5 J=0 R=0	Q=-0.5+0.5i D=1 Γ=.025 S=1 J=.5 R=.1	Q=-.75 D=-1 Γ=1 S=0 J=0 R=3
L	Δ	Δ	Δ	Δ
1.5	.82204+1.5455i	-2.1038+2.8456i	-1.0426+0.1459i	6.7670
2	1.1049+1.3507i	-2.0670+2.8831i	-1.8000+0.2103i	6.7909
2.5	1.1172+1.2938i	-2.0658+2.8832i	-1.7310+0.4847i	6.7904
3	1.1174+1.2937i	-2.0657+2.8832i	-1.6326+0.3954i	6.7904
3.5	1.1174+1.2937i	-2.0657+2.8832i	-1.6730+0.3960i	6.7904

Table 3-2: Four examples of Δ calculated with an increasing endpoint, a fixed spacing of s=0.1 and the asymptotic boundary conditions.

We can see good convergence with little change beyond 2.5 except for the third example.

For comparison we do the same with the more usual (Dirichlet) boundary conditions when trying to approximate a function with finite norm on an infinite range by a function on a finite range i.e.

$h(-L) = 0 \quad y(-L) = 0 \quad h(L) = 0 \quad y(L) = 0$

	Q=1 D=.5 Γ=.25 S=.1 J=2 R=1	Q=i D=1 Γ=1 S=.5 J=0 R=0	Q=-0.5+0.5i D=1 Γ=.025 S=1 J=.5 R=.1	Q=-.75 D=-1 Γ=1 S=0 J=0 R=3
endpoints	Δ	Δ	Δ	Δ
1.5	1.5251+1.0306i	-1.8670+2.8058i	-1.2220+0.7367i	6.2326
2	1.1155+1.2698i	-2.0610+2.8727i	-1.4612+0.1101i	6.6073
2.5	1.1181+1.2937i	-2.0658+2.8831i	-1.8283+0.4064i	6.7904
3	1.1174+1.2938i	-2.0657+2.8832i	-1.6388+0.4356i	6.7904
3.5	1.1174+1.2938i	-2.0657+2.8832i	-1.6642+0.3803i	6.7904

Table 3-3: Four examples of Δ calculated with an increasing endpoint, a fixed spacing of s=0.1 and Dirichlet boundary conditions.

The convergence here is slightly slower. This shows the asymptotic boundary conditions are a slight improvement on the usual ones.

Next we give plots of the four examples when n=250 and L=2.5, which are the typical values we use for the rest of the numerical work.

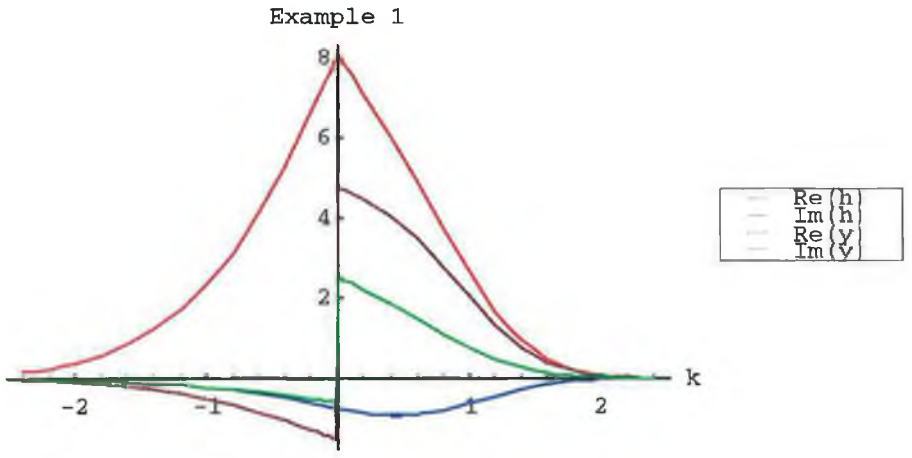

Figure 3-1: Plot of h and y against k for Example 1; Q=1, D=.5, Γ=.25, S=.1, J=2, R=1.

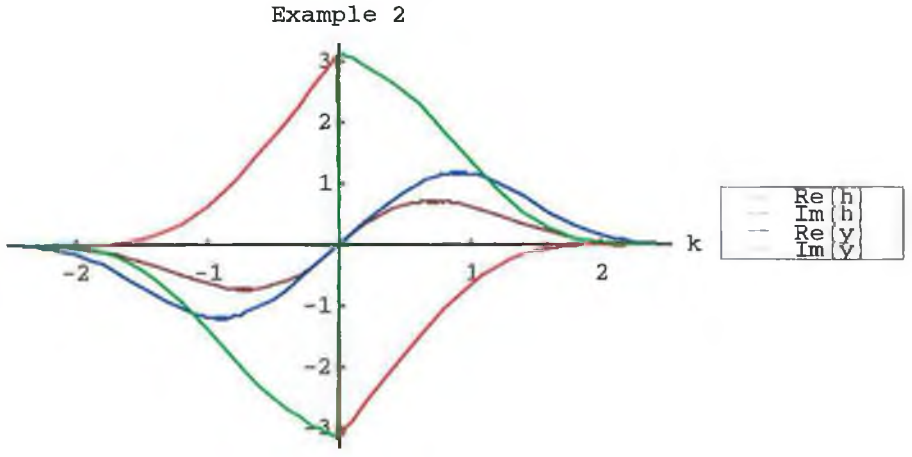

Figure 3-2: Plot of h and y against k for Example 2; Q=i, D=1, Γ=1, J=0, R=0.

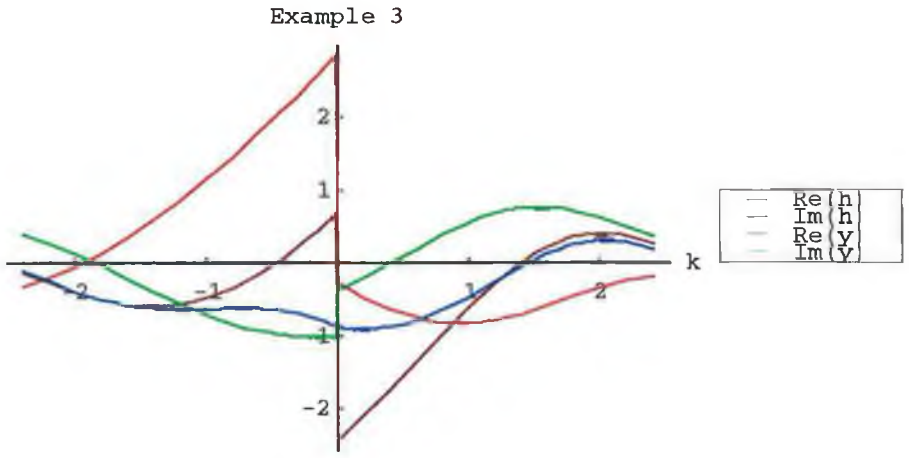

Figure 3-3: Plot of h and y against k for Example 3; Q=-0.5+0.5i, D=1, Γ=0.25, S=1, J=0.5, R=0.1 .

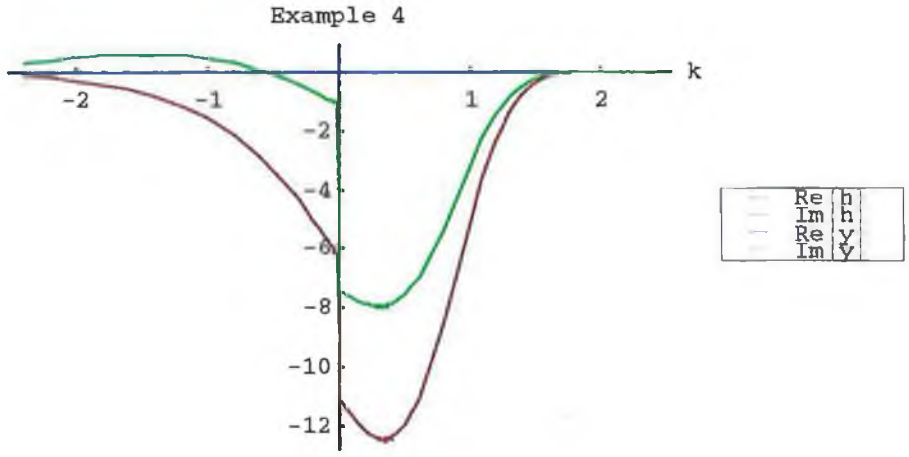

Figure 3-4: Plot of h and y against k for Example 4; Q=-0.75, D=-1, Γ=1, S=0, J=0, R=3.

Solution of $\Delta(Q,...)=\Delta'$

The growth rates for a set of equilibrium parameters are the roots of (3.3). Before using any root-finding schemes it is advised to have a rough idea of the shape of the function you are trying to solve for. This is easiest when J=0. (When J=0 and Q is real, the inhomegeneous parts of the system are all imaginary. Therefore the solutions are imaginary and Δ' is real.)

Muller's method

1 Pick three starting guesses in the complex plain and evaluate at those points.

2. Fit a quadratic through the last three points.

3. Find the roots of the quadratic.

4. The root nearest the last guess becomes the new guess.

5. Evaluate at the new guess

6. Repeat until tolerance is reached

Once we have one root the symmetry properties we discussed earlier enable us to make a good estimate of the second one.

For the second problem we designed a patch which is not fool-proof but works in all but the most extreme cases. From studying the graph above and similar ones we have a rough idea where the right-most singularity is. If the routine takes a relatively large jump past that, we stop the routine. We restart it with a target Δ' that is half way between the last value and our original target. We then restart the routine with our finishing guesses from this detour. In this way we follow a root close to the singularity.

The Critical Matching Parameter Δ_0

For this, we must solve for $\mathrm{Im}(\Delta)=0$ along the imaginary Q axis. Again we draw some graphs to assess any problems we may have in finding a root. We give three examples of Δ plotted along the imaginary Q axis.

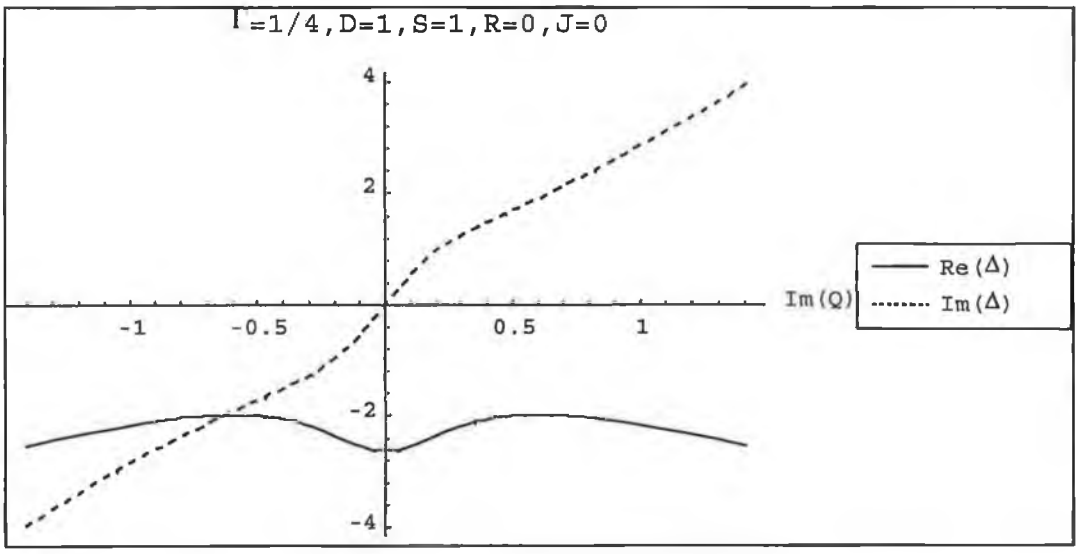

Figure 3-6: Plot of Δ along the line Re(Q)=0 when Γ=1/4,D=1,S=1,R=0,J=0.

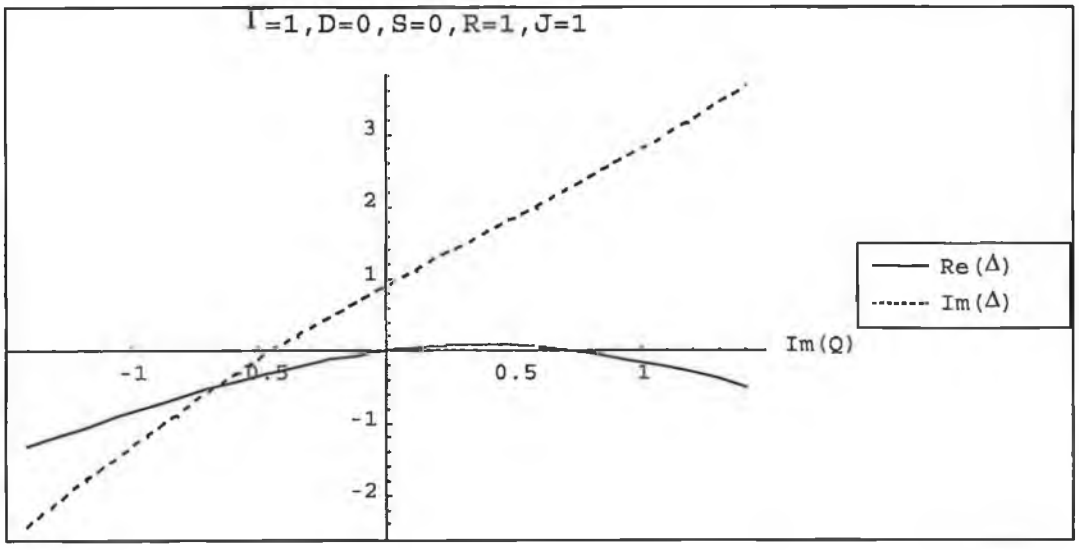

Figure 3-7: Plot of Δ along the line Re(Q)=0 when Γ=1,D=0,S=0,R=1,J=1.

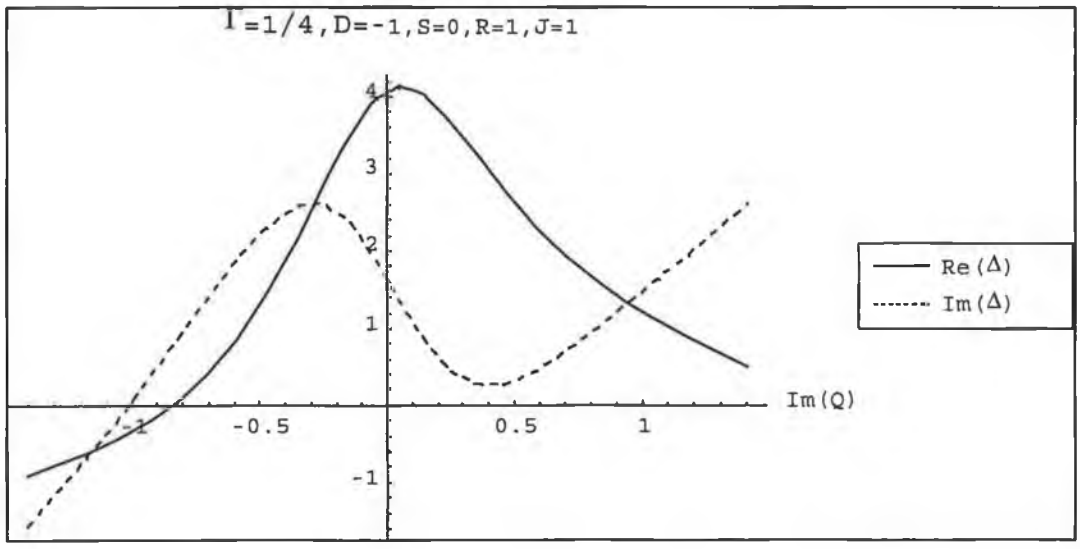

Figure 3-8: Plot of Δ along the line Re(Q)=0 when Γ=1/4,D=-1,S=0,R=1,J=1.

In general there is only one root of Im(Δ)=0. Im(Δ) is almost linear for a large range of the parameters we consider. The second example is not atypical. The main exception is when D<0 where for some values of the equilibrium parameters Im(Δ) develops two turning points and there are potentially three roots. The third example shows such a case.

To cope with this possibility we first sample Δ(Q) at a range of values of Q along the real axis using a small number of elements (64) for each solution of the system. If Im(Δ) changes sign between two of these points we use the secant method and a larger number of elements to locate the root. The actual stability condition is then based on the lowest Re(Δ) corresponding to a root.

4. Series Solutions

In this chapter we consider an alternative approach to the problem. We seek a couple of series solutions to the system, firstly as viscosity tends to infinity and then as flow tends to infinity. We will calculate the coefficients of these series by an adaptation of the code described in the previous chapter. Where possible, we compare our results with those in previous work.

Large Γ

We can scale everything else with respect to viscosity by dividing by the following factors.

k	$\Gamma^{-1/6}$	Γ	Γ	h	$\Gamma^{1/2}$
Q	$\Gamma^{2/3}$	D	Γ	y	$\Gamma^{5/6}$
R	$\Gamma^{1/2}$	J	$\Gamma^{5/6}$	w	$\Gamma^{1/3}$
S	1	Δ'	$\Gamma^{5/6}$		

Table 4-1: Scaling factors for the large Γ series.

These factors were given by Bondeson and Persson (1986) pp. 2999 in a different context. Because S does not scale with viscosity, we will repeat the expansion for different values of S rather than try to include it in the expansion. In terms of the new variables, the system becomes

$$\begin{pmatrix} h'' + k^4 h + y \\ iw' - k^2 y - Sh \\ iy' + k^2 w \end{pmatrix} - Q\begin{pmatrix} k^2 h \\ 0 \\ w \end{pmatrix} - R\begin{pmatrix} -(k^2 h)' \\ 0 \\ w' \end{pmatrix} = Q\begin{pmatrix} 2\pi i\delta' \\ 0 \\ 0 \end{pmatrix} + J\begin{pmatrix} 2\pi\delta \\ 0 \\ 0 \end{pmatrix} + R\begin{pmatrix} 0 \\ S2\pi i\delta \\ 0 \end{pmatrix} + D\begin{pmatrix} 0 \\ 0 \\ 2\pi i\delta \end{pmatrix}. \tag{4.1}$$

As viscosity tends to infinity Q,R,J, and D become small parameters. We note that there is no zero order solution.

We can now build up a regular perturbation for the solution of the form

$$
\begin{aligned}
h = {} & Qh_Q + Q^2 h_{Q^2} + QRh_{QR} \ldots \\
& + Jh_J + JQh_{JQ} + JRh_{JR} \ldots \\
& + Dh_D + DQh_{DQ} + DRh_{DR} \ldots \\
& + Rh_R + RQh_{RQ} + R^2 h_{R^2} \ldots
\end{aligned}
\tag{4.2}
$$

This will be a valid approximation when Γ is large.

Because of the symmetry of these equations it is useful to consider the parity of the perturbations (h's). By even parity we mean even h, even y and odd w and vice versa for odd parity. Of the initial (inhomogeneous) perturbations h_Q and h_D will be odd and h_J and h_R will be even. From there a Q-perturbation maintains the parity and R-perturbation switches it. This is important because only the odd part of h contributes to the matching parameter. Also notice that only the J perturbations are real and therefore the corresponding matching parameters will be imaginary. Therefore

$$
\begin{aligned}
\Delta' = {} & \Delta_Q Q + \Delta_{Q^2} Q^2 \ldots \\
& + \Delta_D D + \Delta_{DQ} DQ \ldots \\
& + \Delta_{JR} JR \ldots \\
& + \Delta_{R^2} R^2 \ldots
\end{aligned}
\tag{4.3}
$$

or in terms of the unscaled variables

$$
\begin{aligned}
\frac{\Delta'}{\Gamma^{5/6}} = {} & \Delta_Q \frac{Q}{\Gamma^{2/3}} + \Delta_{Q^2} \frac{Q^2}{\Gamma^{4/3}} \ldots \\
& + \Delta_D \frac{D}{\Gamma} + \Delta_{DQ} \frac{DQ}{\Gamma^{5/3}} \ldots \\
& + \Delta_{JR} \frac{JR}{\Gamma^{4/3}} \ldots \\
& + \Delta_{SR^2} \frac{SR^2}{\Gamma} \ldots
\end{aligned}
\tag{4.4}
$$

Next we give numerical results in correct Γ order.

Term	Order in Γ^{-1}	S=0	S=.1	S=.25	S=.5	S=1
Q	-1/6	2.1035	2.1088	2.1165	2.1294	2.1545
D	1/6	-2.1824	-2.17926	-2.1746	-2.1670	-2.1520
R^2		0	.0759	0.1383	.1513	-0.0084
JR	1/2	.9497i	.7501i	.5076i	.2046i	-0.1957i
Q^2		.4166	.4564	0.5156	.6127	.8015
DQ	5/6	1.1715	1.1854	1.2059	1.2394	1.3037
QR^2		.2248	.1631	0.1593	0.2565	0.6036
DR^2	7/6	-0.5163	-0.4169	-0.2918	-0.1307	.0959
R^4		0	.0100	-0.0194	-0.0235	-.0047
JRQ		-.8375i	.5725i	-.2873i	.0160i	0.3387i
Q^3		-0.0851	-.1256	-.18628	-.3112	-.5047
remaining terms	3/2					

Table 4-2: Numerical values of the coefficients of the large Γ series for Δ.

In Coppi et al. (1966) the equivalent values given when S=0 are for the Q term 2.104 and for the D term -2.198.

By writing Q as a Taylor Series in $\Gamma^{-1/6}$ and matching terms of the same order we can form a series for Q. (The manipulations were done using Mathematica.)

The series starts like

$$Q = \frac{\Delta'}{\Delta_Q}\Gamma^{-1/6} + \frac{\Delta_D}{\Delta_Q}\Gamma^{-1/3} + \frac{\Delta_{JR}JR}{\Delta_Q}\Gamma^{-1/2} - \frac{\Delta_{Q^2}\Delta^2}{\Delta_Q^3}\Gamma^{-1} - \frac{2\Delta_D\Delta_{Q^2}D\Delta}{\Delta_Q^3}\Gamma^{-7/6} - \frac{\Delta_{DQ}D\Delta}{\Delta_Q^2}\Gamma^{-7/6} - \frac{\Delta_{QR^2}R^2\Delta}{\Delta_Q^2}\Gamma^{-7/6}\ldots \quad (4.5).$$

Note that as viscosity tends to infinity the growth time tends to zero as would be expected.

Term	Order in Γ^{-1}	S=0	S=.1	S=.25	S=.5	S=1
Δ'	1/6	0.4754	0.4748	0.4725	0.4696	0.4641
D	1/3	1.0375	1.0354	1.0274	1.0176	0.9989
R^2		0	-0.0360	-0.0654	-0.0711	0.0038
JR	2/3	-0.4515i	-0.3557i	-0.2398i	-0.0961i	0.0889i
Δ^2	1	-.00942	-0.1026	-0.1151	-0.1351	-0.1727
ΔD	7/6	-0.4602	-0.4787	-0.5057	-0.5484	-0.6258
ΔR^2		-0.0508	-0.0293	-0.0205	-0.0373	-0.1314
D^2	4/3	-0.1294	-0.0935	-0.0411	0.0422	0.1953
DR^2		0.0237	0.1321	0.1547	0.0026	-0.6143
R^4		0	0.0129	0.0255	0.0337	0.0033
other terms	3/2					

Table 4-3: Numerical values of the coefficients of the large Γ series for Q.

We can see that the first two terms do not vary greatly with S. In fact S slightly stabilises these terms. The JR term is suppressed by S. Also notice that this term only affects the complex part of the growth time. In fact the effect of J on the real part of the growth time will not appear until the series reaches terms of order Γ^{-2}. This effect dominates the results for the viscous slab. Not all of the other terms are particularly significant as they are of roughly the same order as some of the numerical errors of the previous chapter. Those that are significant display a curious dependence on S.

Large R

A similar process can be followed if we scale everything with respect to R. This expansion will be valid when R is large (but not so large as to break the ordering). The appropriate factors are

k	$R^{-1/3}$	Γ	R^2	h	R
Q	$R^{4/3}$	D	R^2	y	$R^{5/3}$
R	R	J	$R^{5/3}$	w	$R^{2/3}$
S	1	Δ'	$R^{5/3}$		

Table 4-4: Scaling factors for the large R series.

In terms of the new variables the system becomes:

$$\begin{pmatrix} h''+(k^2h)'+y \\ iw'-k^2y-Sh \\ iy'-w' \end{pmatrix} - Q\begin{pmatrix} k^2h \\ 0 \\ w \end{pmatrix} - \Gamma\begin{pmatrix} k^4h \\ 0 \\ k^2w \end{pmatrix} =$$

$$Q\begin{pmatrix} 2\pi i\delta' \\ 0 \\ 0 \end{pmatrix} + J\begin{pmatrix} 2\pi\delta \\ 0 \\ 0 \end{pmatrix} + \underline{\begin{pmatrix} 0 \\ S2\pi i\delta \\ 0 \end{pmatrix}} + D\begin{pmatrix} 0 \\ 0 \\ 2\pi i\delta \end{pmatrix}$$

(4.6)

As R tends to infinity Q,Γ, J and D become small parameters. The symmetry properties we discussed earlier are not applicable here but the discussion about the comments about the J-perturbations being imaginary still holds true.

There will be two cases S=0 and S>0. We will see that we get different behaviours in the two cases.

Case I: S>0

Here we must split the two parts of the effective driving term $D+SR^2$ as they scale differently with R. As R tends to infinity so does the effective driving term. This means we are tending towards the slow interchange ordering.

Unlike the other expansion there is a zero order solution in this case because of the underlined term which does not tend to zero as R tends to infinity. There is also a zero order growth time, Q_0, when $\Delta=0$. To find this growth time we use the code as described in the last chapter.

About these growth times we can take perturbations in the corresponding manner to the previous section. We can then generate a series for Q, in an equivalent manner to the previous section, which starts

$$Q = Q_0 R^{\frac{4}{3}} + \frac{\Delta' - \Delta_J J}{\Delta_Q} R^{-\frac{1}{3}} + \frac{\Delta_D D + \Delta_\Gamma \Gamma}{\Delta_Q} R^{-\frac{2}{3}} \ldots \qquad (4.7).$$

Next we give the numerical values of these terms.

Term	Order in R^{-1}	S=0.001	S=0.01	S=0.1	S=0.25	S=0.5	S=1
Q_0	-4/3	0.036	0.110	0.327	0.491	0.651	0.836
Δ	1/3	2.358	0.847	0.385	0.312	0.278	0.258
J		-6.768i	-2.009i	-0.496i	-0.223i	-0.081i	0.019i
D	2/3	16.676	4.676	1.257	0.776	0.566	0.437
Γ		-7.198	-5.836	-3.688	-2.771	-2.162	-1.673
remaining terms	2						

Table 4-5: Numerical values of the coefficients of the large R series for Q when S>0.

As we can see the J term is suppressed by S as was the case in the large viscosity expansion. The D term is also stabilised by S. The zero order growth time, Q_0, rises quite sharply with low S.

Case II: S=0

In this case we do not have a zero order solution or a zero order growth time so we may proceed in an identical fashion to how we approached large Γ. We are aided by the fact that we can compare results with those for work in the slab in Hou (1994). This work was done analytically and the results given in closed form. The numerical results we get are

Δ terms	Order in R^{-1}		Slab
Q	-1/3	-0.005	0
J	0	3.144	3.142
D	1/3	-8.083	N/A
Q^2	1	6.285	6.284
JQ	4/3	-8.067	•
DQ	5/3	20.113	N/A
$Q\Gamma$		11.643	•
$J\Gamma$	2	-14.933	•
Q^3	7/3	-16.087	•
$D\Gamma$		6.788	N/A
remaining terms	8/3		

Table 4-6: Numerical values of the coefficients of the large R series for Δ when S=0 (and comparisons with Hou (1994)).

(N/A indicates no comparison with slab. • indicates comparison was possible but not carried out.)

We would like to continue in the same manner as before but we would be dividing by Δ_Q, which vanishes. The lowest term involving Q is now the Q^2 term. To start the series we balance that term with the lowest terms not involving Q.

$$\begin{aligned}
&(\Delta' - \Delta_J J)R^{-\frac{5}{3}} = \Delta_{Q^2} Q^2 R^{-\frac{8}{3}} \\
&\frac{\Delta' - \Delta_J J}{\Delta_{Q^2}} R = Q^2 \qquad (4.8). \\
&\pm\sqrt{\frac{\Delta' - \Delta_J J}{\Delta_{Q^2}}} R^{\frac{1}{2}} = Q
\end{aligned}$$

Again we try to match terms but in this case we write Q as a series in powers of $R^{-1/6}$, i.e. $Q = \sum_{i=-3}^{\infty} b_i R^{-\frac{1}{6}i}$. We can then substitute that series in and match the corresponding powers of R. We then get

$$\begin{aligned}
Q = \pm\sqrt{\frac{\Delta' - \Delta_J J}{\Delta_{Q^2}}} R^{\frac{1}{2}} \mp \frac{\Delta_D D}{2\sqrt{\Delta_{Q^2}}\sqrt{\Delta' - \Delta_J J}} R^{\frac{1}{6}} \mp \frac{\Delta_D^2 D^2}{8\sqrt{\Delta_{Q^2}}(\Delta' - \Delta_J J)^{\frac{3}{2}}} R^{-\frac{1}{6}} \\
- \frac{\left(\Delta_{JQ} - \Delta_J \Delta_{Q^3}\right)}{2\left(\Delta_{Q^2}\right)^2} R^{-\frac{1}{3}} - \frac{\Delta_{Q^3}\Delta'}{2\left(\Delta_{Q^2}\right)^2} R^{-\frac{1}{3}} \ldots
\end{aligned}$$

(4.9).

Because we are working with the Q^2 term we get the two roots closest to zero.

Next we give the numerical values

Terms	Order in R^{-1}	Order in $\sqrt{\Delta + \Delta_J J}$	Q	Slab
1	-1/2	1	0.399	0.399
D	-1/6	-1	-1.612	N/A
D^2	1/6	-3	3.258	N/A
J	1/3	0	0.002	0
Δ'		0	0.204	0.205
D^3	1/2	-5	-13.167	N/A
D	2/3	0	0.236	N/A
Γ		0	-0.926	-0.939

Table 4-7: Numerical values of the coefficients of the large R series for Q when S=0.

$(\Delta + \Delta_J J$ is vital for the growth rate of the mode in this case. Unless J=0 and $\Delta'<0$ one of the square roots in the first term will have a positive real part. As R tends to infinity this will dominate and the mode will definitely be unstable. The interaction between D and $\Delta'+\Delta_J J$ is quite complicated. If $D/(\Delta'+\Delta_J J)$ is large the convergence of the series will be quite slow. We will see from the results section that this interaction can give rise to the curious result that decreasing the driving term can destabilise modes for large fixed R. The dominant factor in the stability of the tearing mode is still the matching parameter, $\Delta`$, and decreasing $\Delta`$is always stabilising.

In the limit as R tends to infinity the two cases are distinct. For moderate R there will be a blurring of the boundary between the cases. For small S the behaviour will correspond more to the second case than the first.

5. Numerical Results

General Comments

We can say some things about the results in general.

When S=0:

When D=0, the results confirm the results from the slab as expected. When J=0, R has a small destabilising effect. The interaction of J and R is destabilising. The effects of D and G though seem to be quite different. This is not unexpected and was pointed out in the conclusion in Coppi et al. (1966).

When S>0:

When R=0, S has little effect, confirming the results in Coppi et al. (1966).

S suppresses the destabilising effect of J. The key effect is that the driving term becomes $(D+SR^2)$. After that the situation becomes more confused.

Plots of Re(Q) against R

Firstly we will give some examples of Re(Q) against R for various values of the parameters.

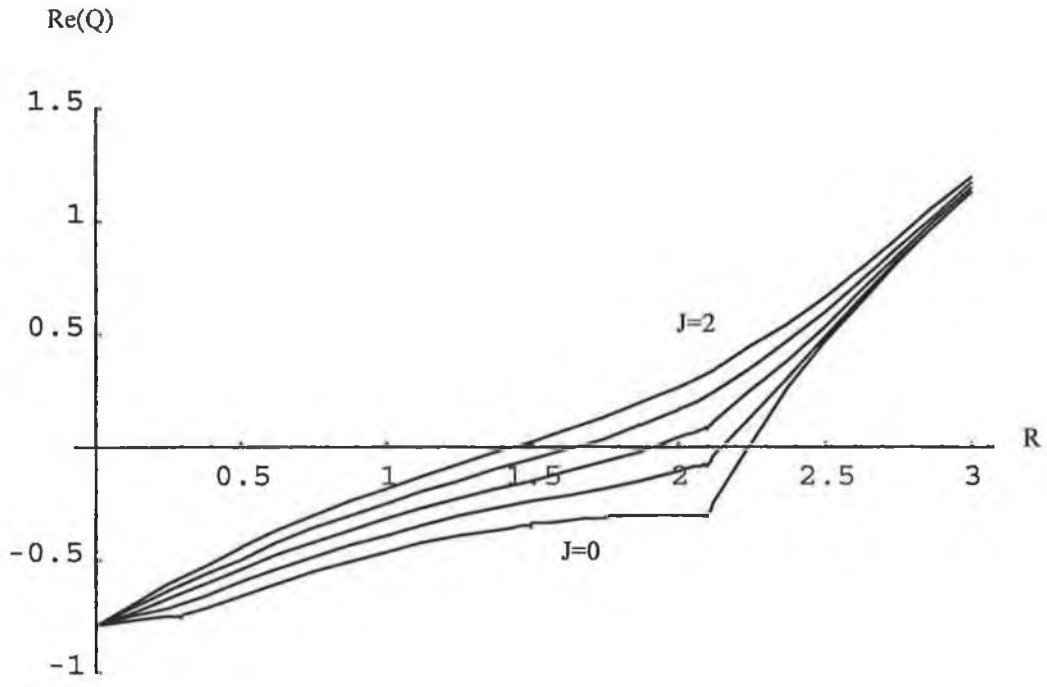

Figure 5-1: Plot of Re(Q) against R for Γ=1/2,S=1/4,D=-1,Δ′=-1 and J=0,0.5,1,1.5,2

At R=2 the effective driving term changes sign and there is a change in behaviour. The current, J, becomes less important after this change in behaviour.

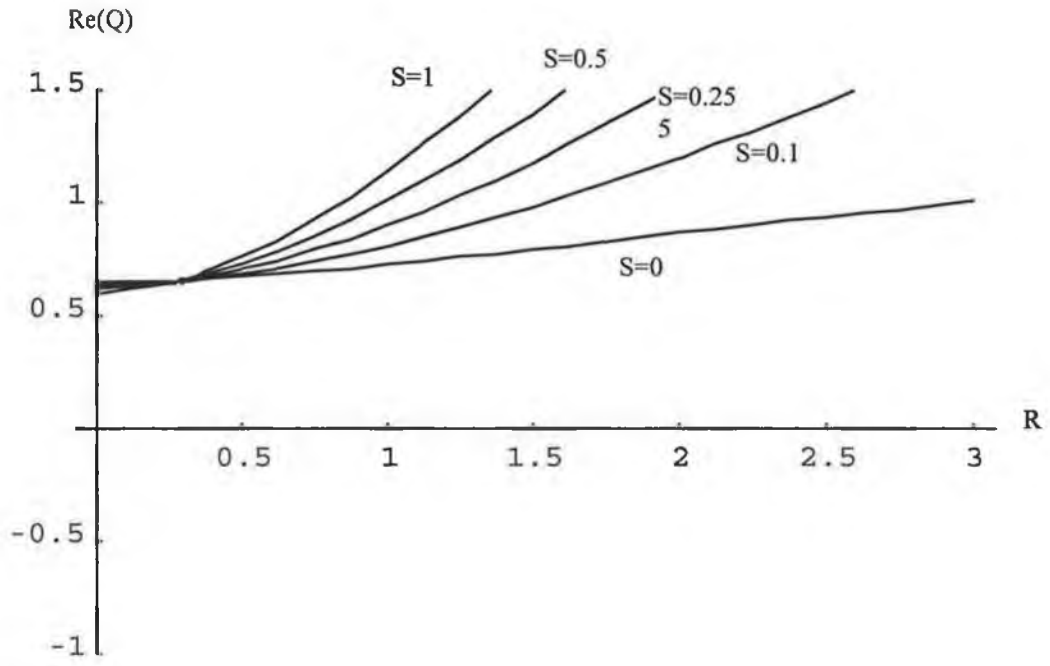

Figure 5-2: Graph of Re(Q) against R for Γ=1/2,D=1/4,J=1,Δ′=1 and S=0,0.1,0.25,0.5,1

The change in effective driving term is clearly visible here.

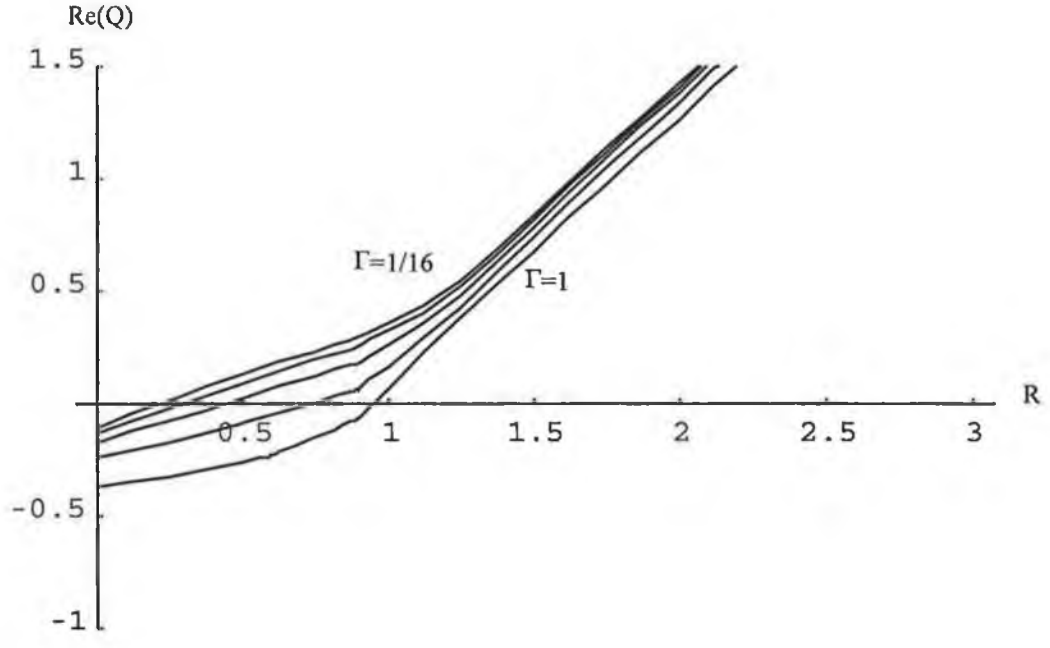

Figure 5-3: Graph of Re(Q) against R for S=1/2,D=-1,Δ′=1,J=2 and Γ=1/16,1/8,1/4,1/2,1.

As the effective driving term rises, the effect of viscosity becomes less significant.

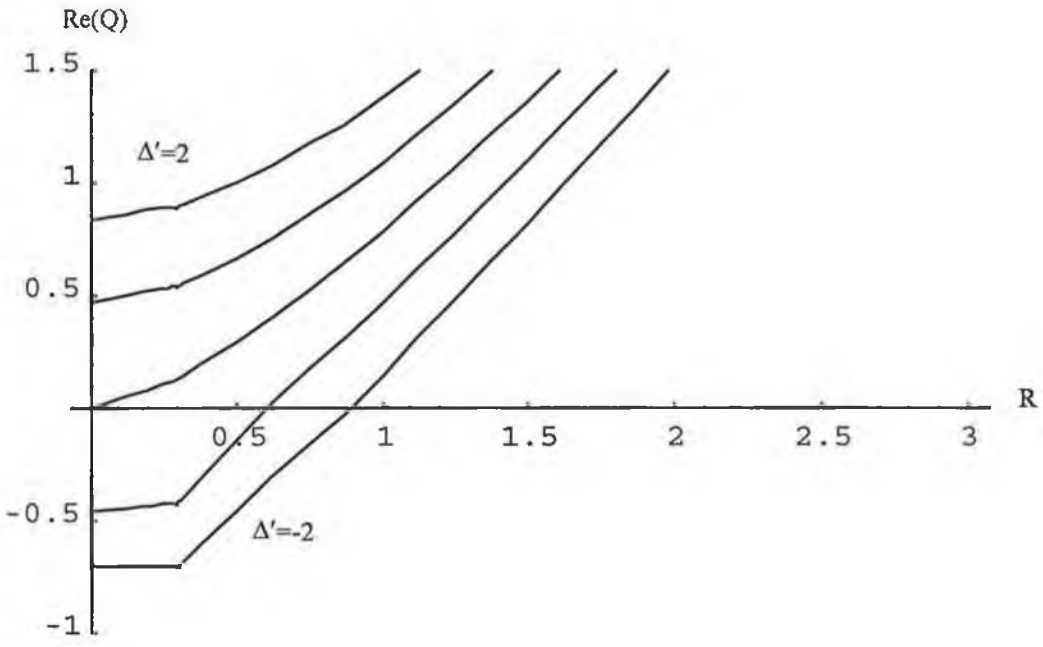

Figure 5-4: Graph of Re(Q) against R for Γ=1/2, S=1, D=0, J=0 and Δ′=-2,-1,0,1,2.

The flattening off of the curves at R=0 for $\Delta'<0$ is due to the change from a complex root to a real root.

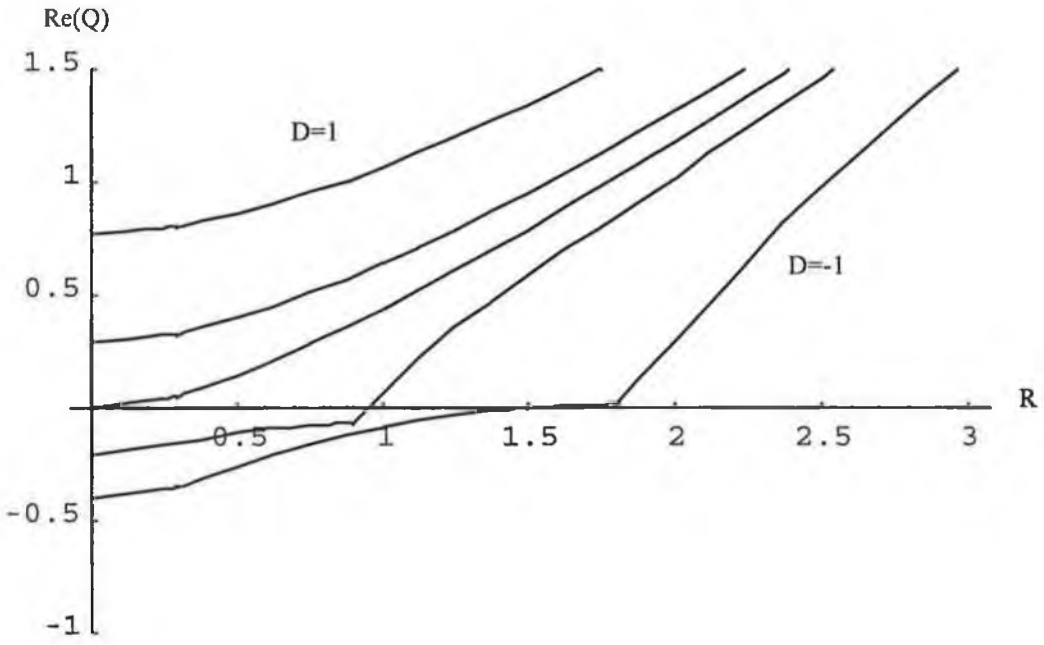

Figure 5-5: Graph of Re(Q) against R for Γ=1/8,S=1/4,J=0,Δ′=0 and D=-1,-1/4,0,1/4,1.

The changes in behaviour here occur as the effective driving term changes sign. The flattening of the curves for D<0 occurs as the roots change from complex to real.

As we can see, flow is in general destabilising. We can also see that the effective driving term dominates the other parameters.

Critical Value, Δ_0, Plots

This is our main body of results. These contour plots show the critical value of the matching parameter, Δ_0, for varying values of S and R. For each graph 121 values of Δ_0 were calculated for 11 points between S=0 and S=1 inclusive and 11 points between R=0 and R=3 inclusive. The gap between contours is 0.5. There are twelve of them for a combination of values of Γ, D_R, and J. If we were to hold D constant for these graphs the change in the effective driving term would dominate, so instead we hold $D_R = D+SR^2$ constant. By peeling off the dominant effect, we are able to see other effects more clearly.

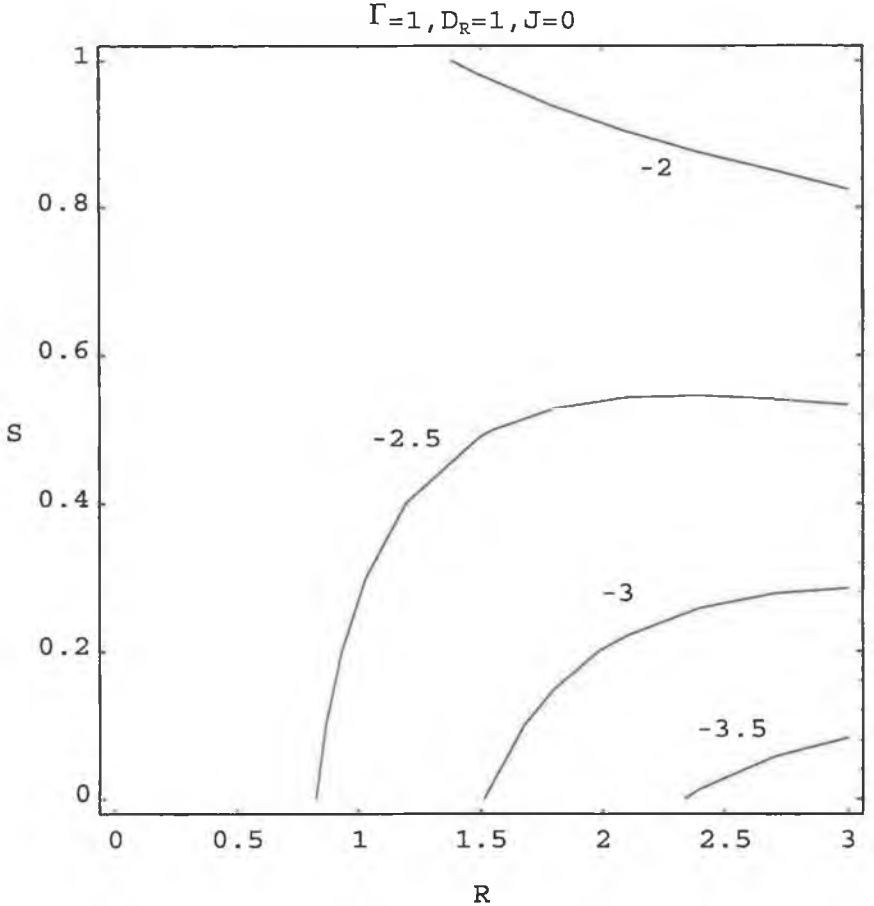

Figure 5-6: Contour Plot of Δ_0 for R[0,3] S[0,1] Γ=1, D_R=1, J=0. Increasing flow, R, with low S destabilises the modes. Increasing flow, R, with high S stabilises the modes so the change in driving term with high S and R is slightly self-suppressed.

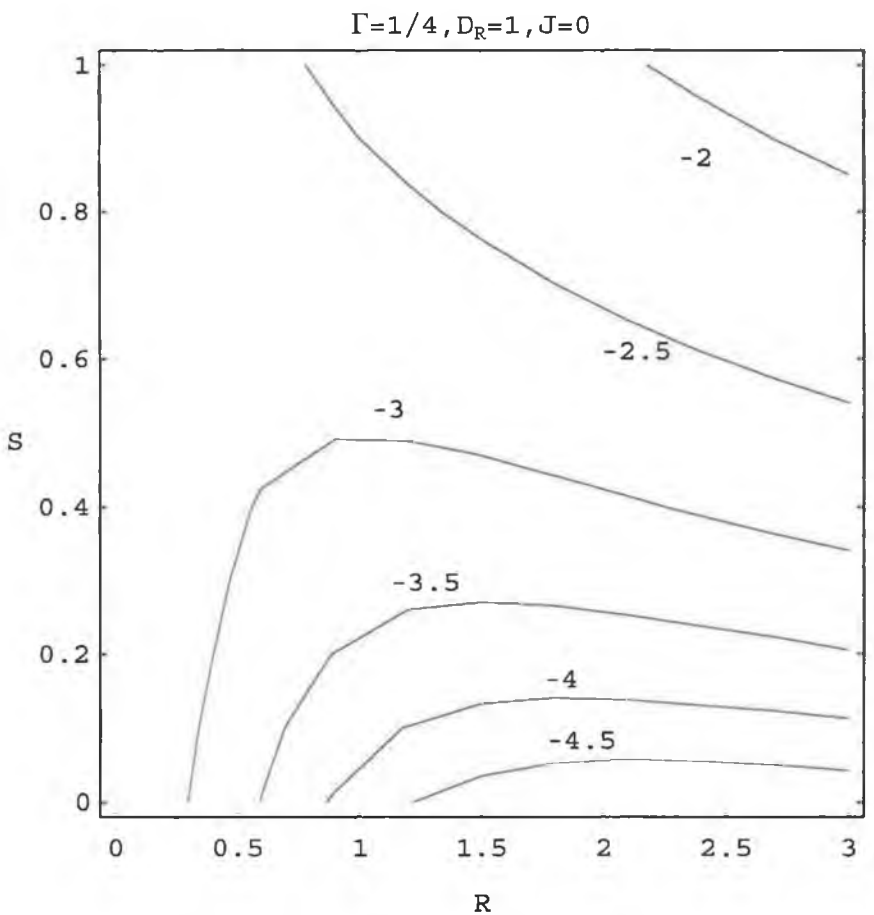

Figure 5-7: Contour Plot of Δ_0 for R[0,3] S[0,1] Γ=1/4, D_R=1, J=0. The comments from the last graph still apply here. As expected reducing viscosity further destabilises the modes except in the top right-hand corner of the graph.

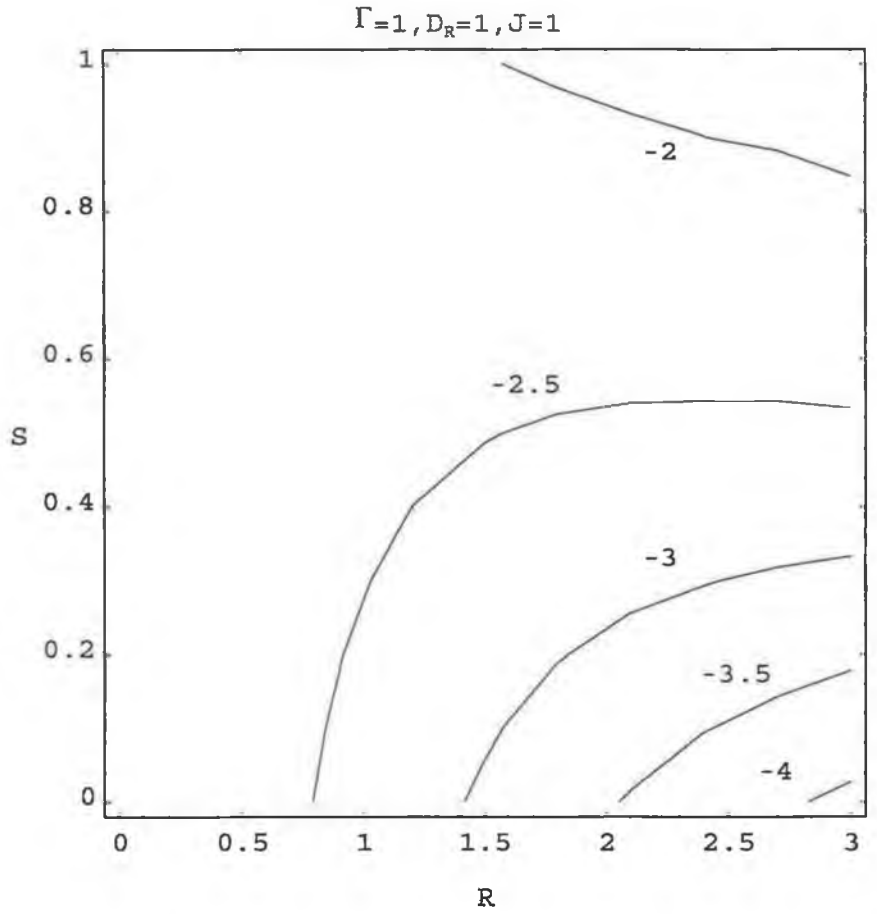

Figure 5-8: Contour Plot of Δ_0 for R[0,3] S[0,1] Γ=1, D_R=1, J=1. The effect of the interaction between R and J seems to be dominated by the driving term and is hardly noticeable.

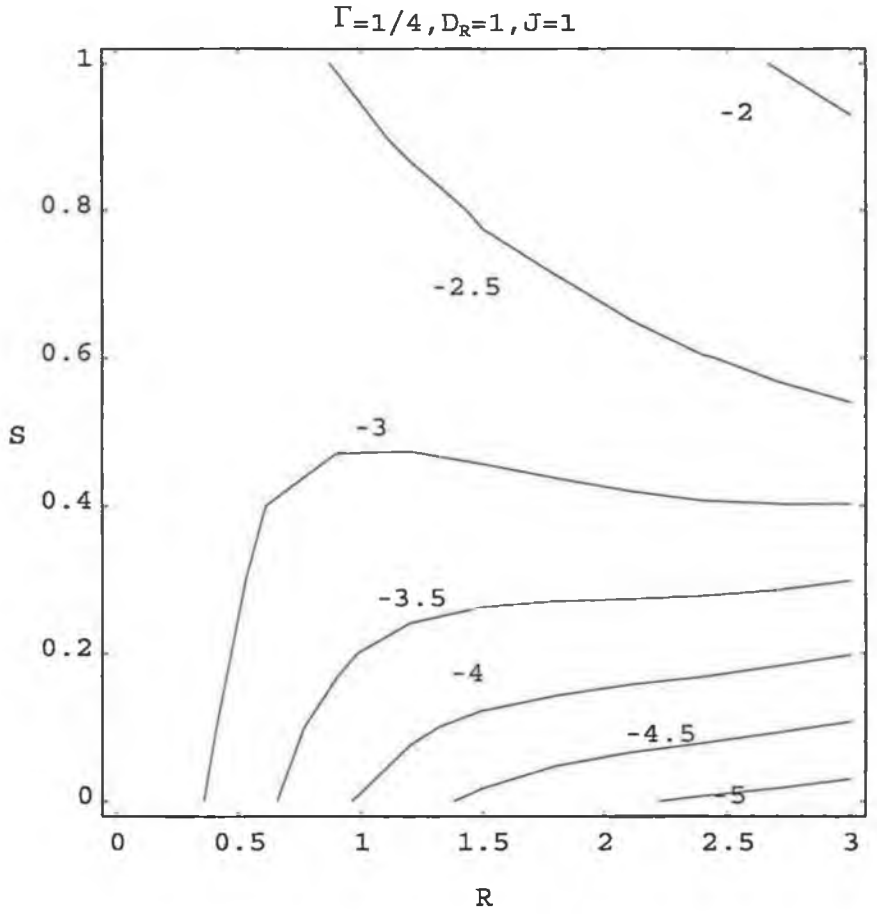

Figure 5-9: Contour Plot of Δ_0 for R[0,3] S[0,1] Γ=1/4, D_R=1, J=1. The comments from the previous graph apply here.

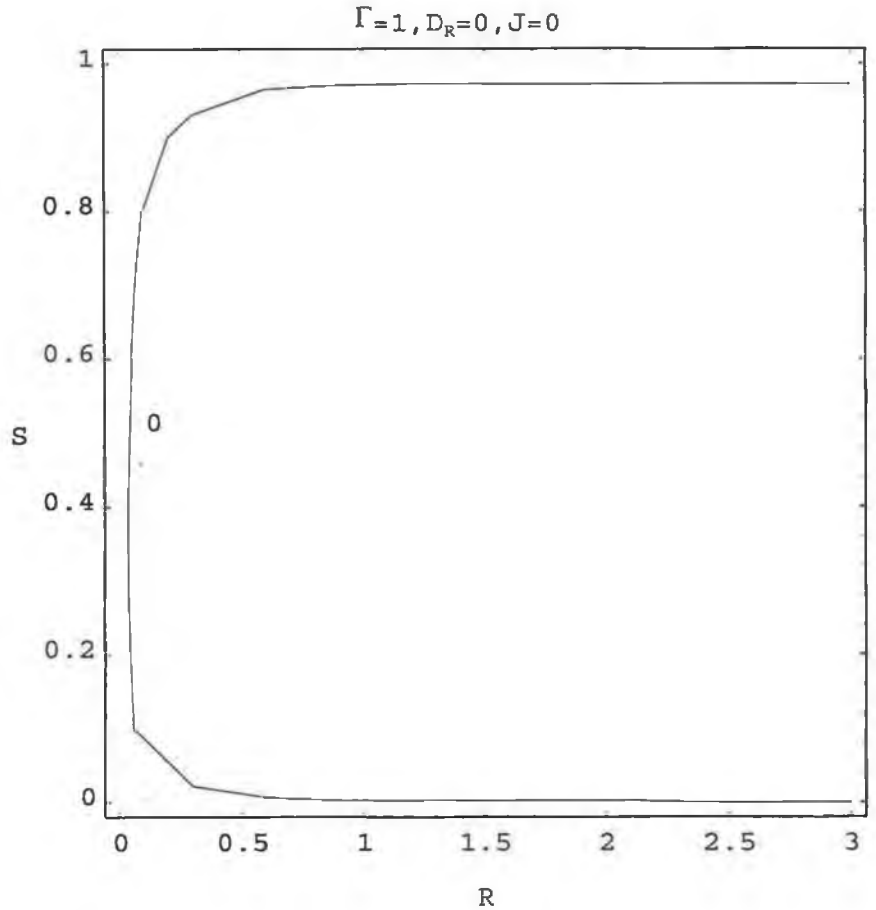

Figure 5-10: Contour Plot of Δ_0 for R[0,3] S[0,1] Γ=1, D_R=0, J=0. Without D_R or J, flow has very little effect. The variation is so small it does not show up on the scale we are using. The minimum of Δ_0 on this graph is -0.35 and occurs when S=0.3 and R=3.

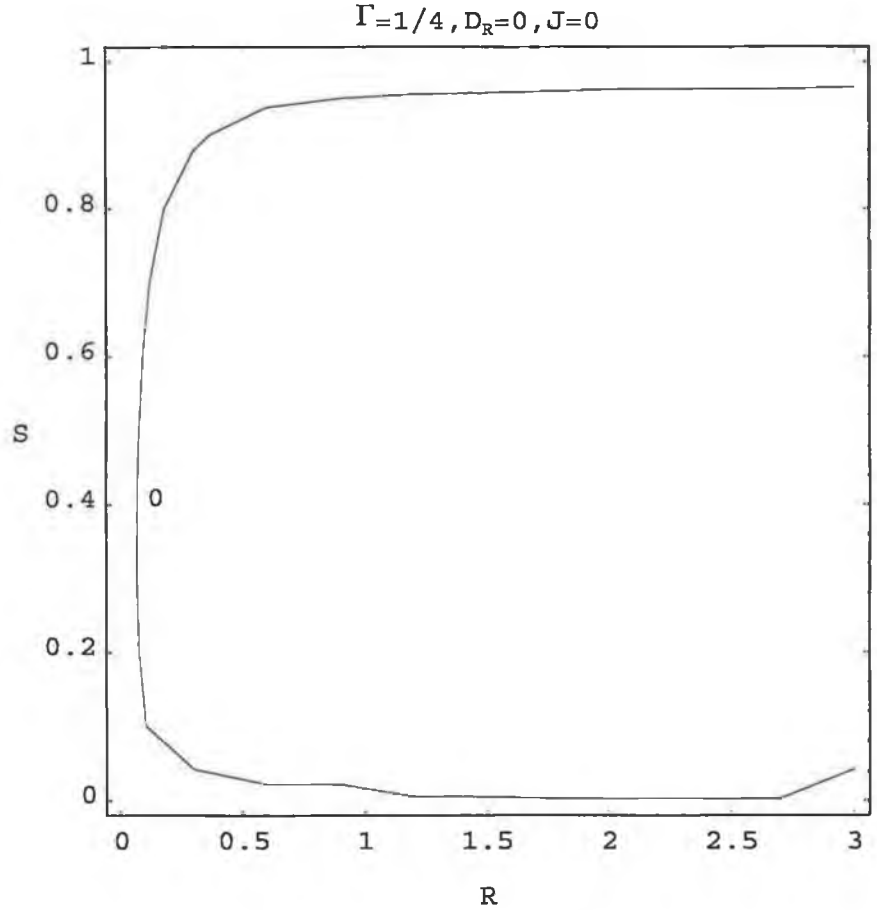

Figure 5-11: Contour Plot of Δ_0 for R[0,3] S[0,1] Γ=1/4, D_R=0, J=0. The minimum of Δ_0 on this graph is -0.27 and occurs when S=0.3 and R=2.7

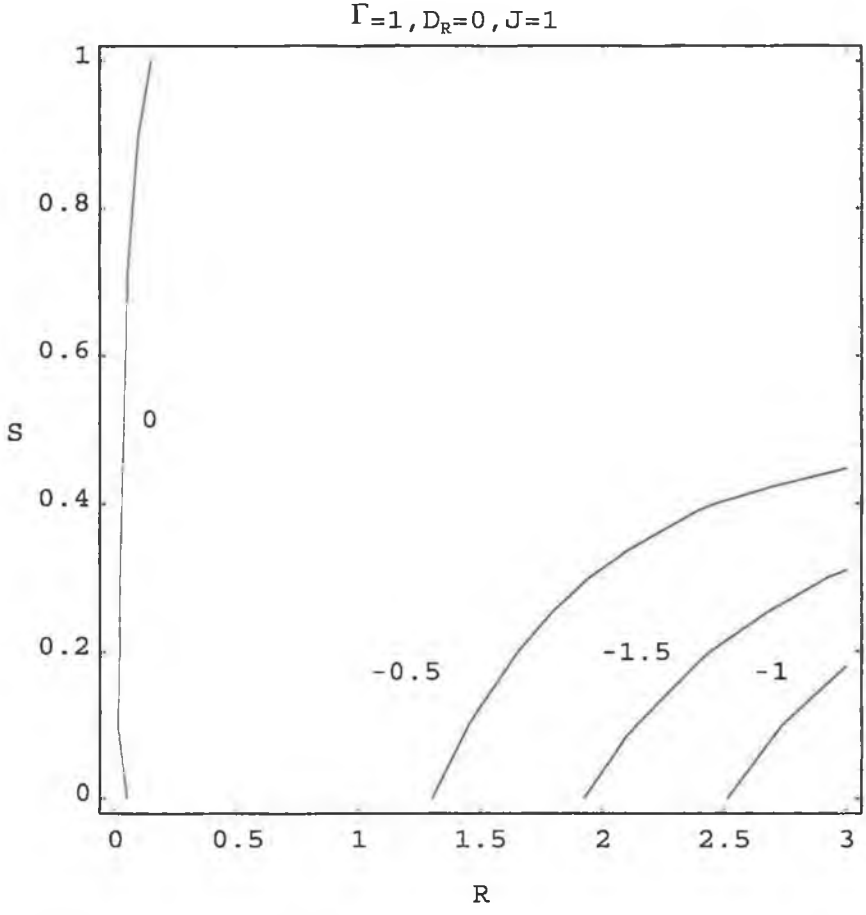

Figure 5-12: Contour Plot of Δ_0 for R[0,3] S[0,1] Γ=1, D_R=0, J=1. Here we can see the destabilising effect of the interaction between R and J when S is low.

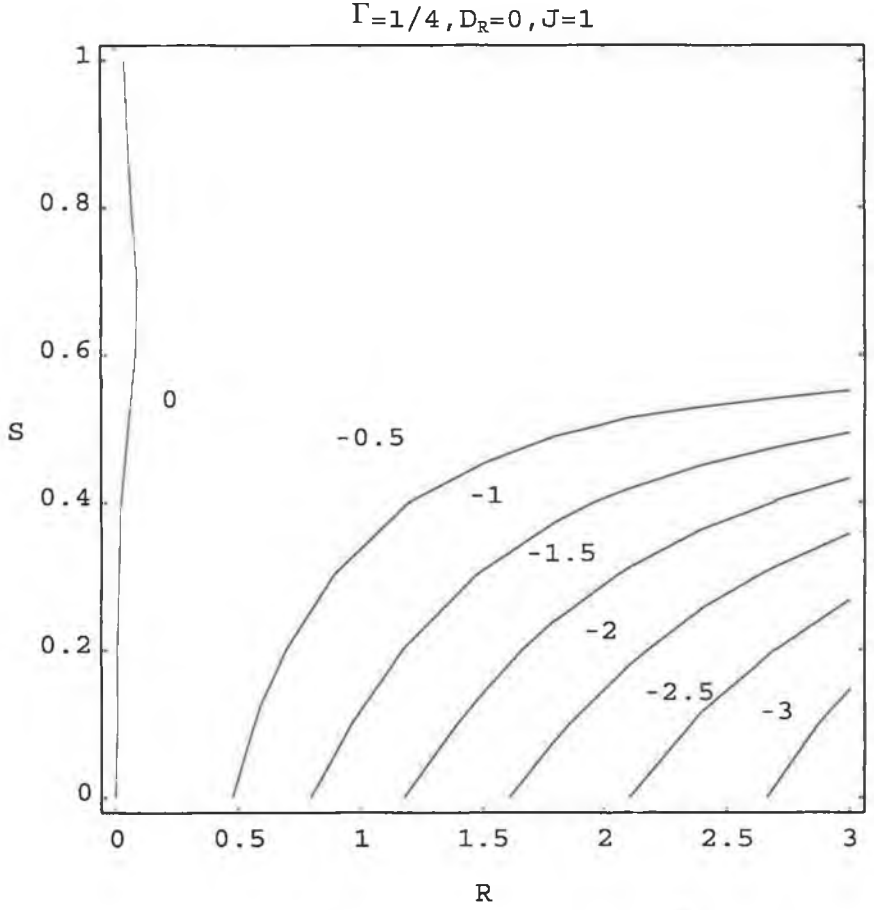

Figure 5-13: Contour Plot of Δ_0 for R[0,3] S[0,1] Γ=1/4, D_R=0, J=1. With low viscosity this interaction is even more destabilising.

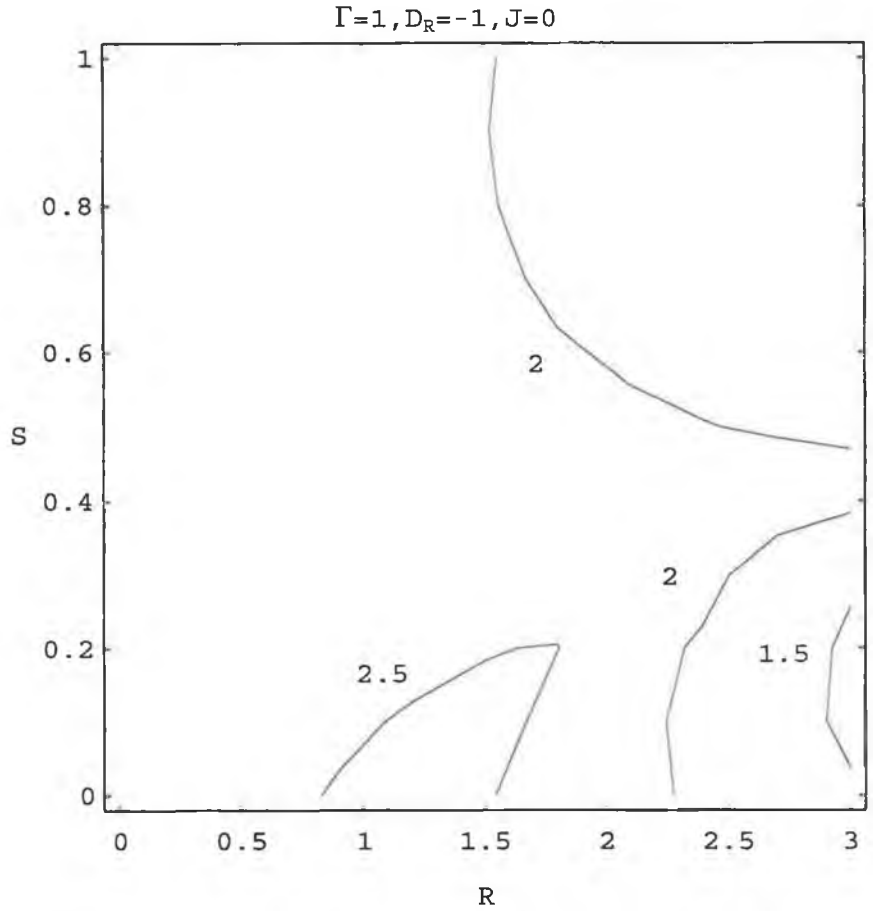

Figure 5-14: Contour Plot of Δ_0 for R[0,3] S[0,1] Γ=1, D_R=-1, J=0. For low S, R is initially stabilising and then is destabilising. This change occurs as a different mode becomes critical. For high S, R is destabilising.

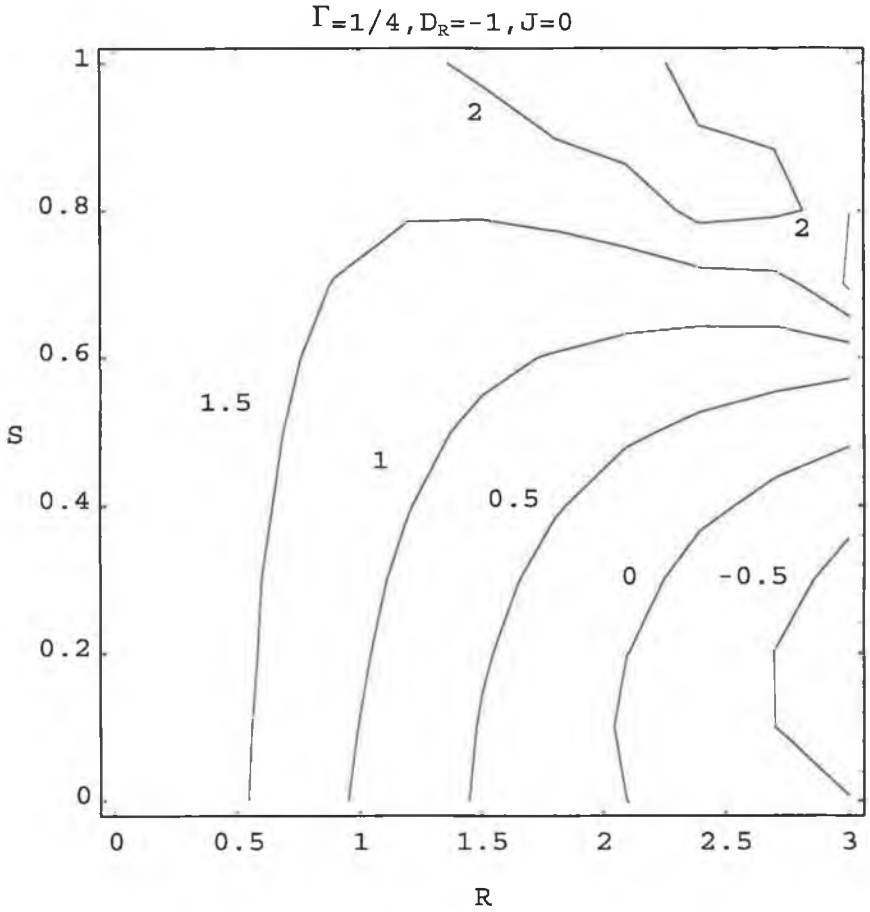

Figure 5-15: Contour Plot of Δ_0 for R[0,3] S[0,1] Γ=1/4, D_R=-1, J=0.

In the bottom right-hand corner of this graph we see a curious effect. Decreasing the driving term has destabilised the mode when we compare it with the equivalent graph for D_R=0.

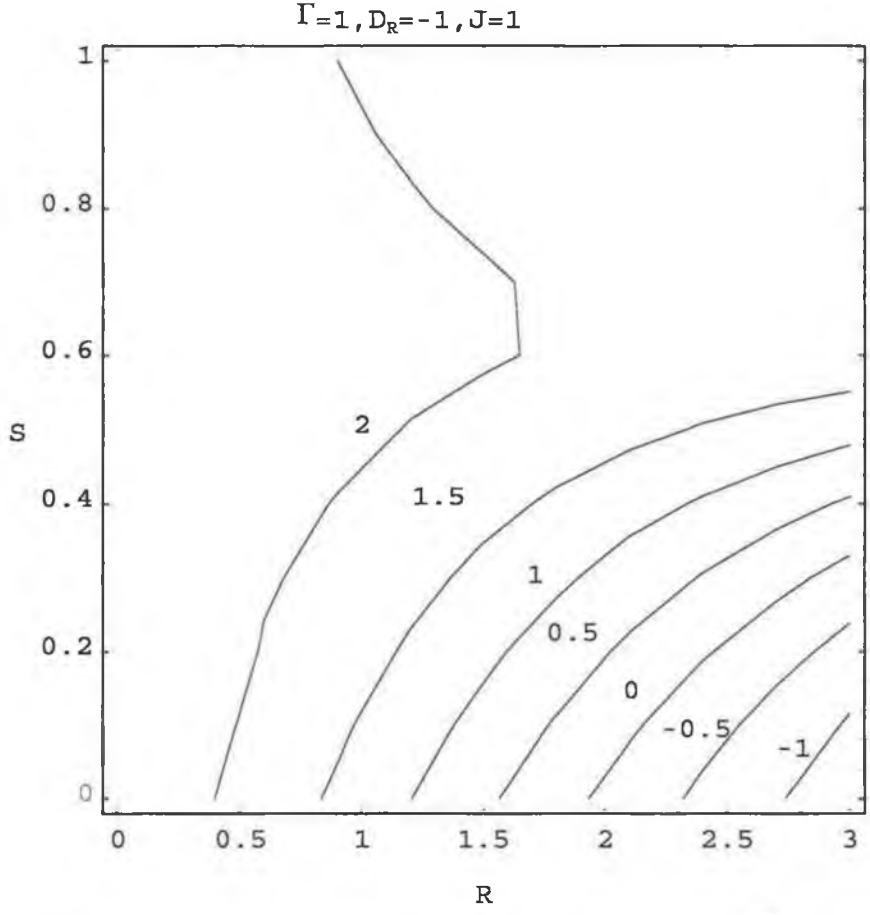

Figure 5-16: Contour Plot of Δ_0 for R[0,3] S[0,1] Γ=1, D_R=-1, J=1. Again we see the interaction between R and J.

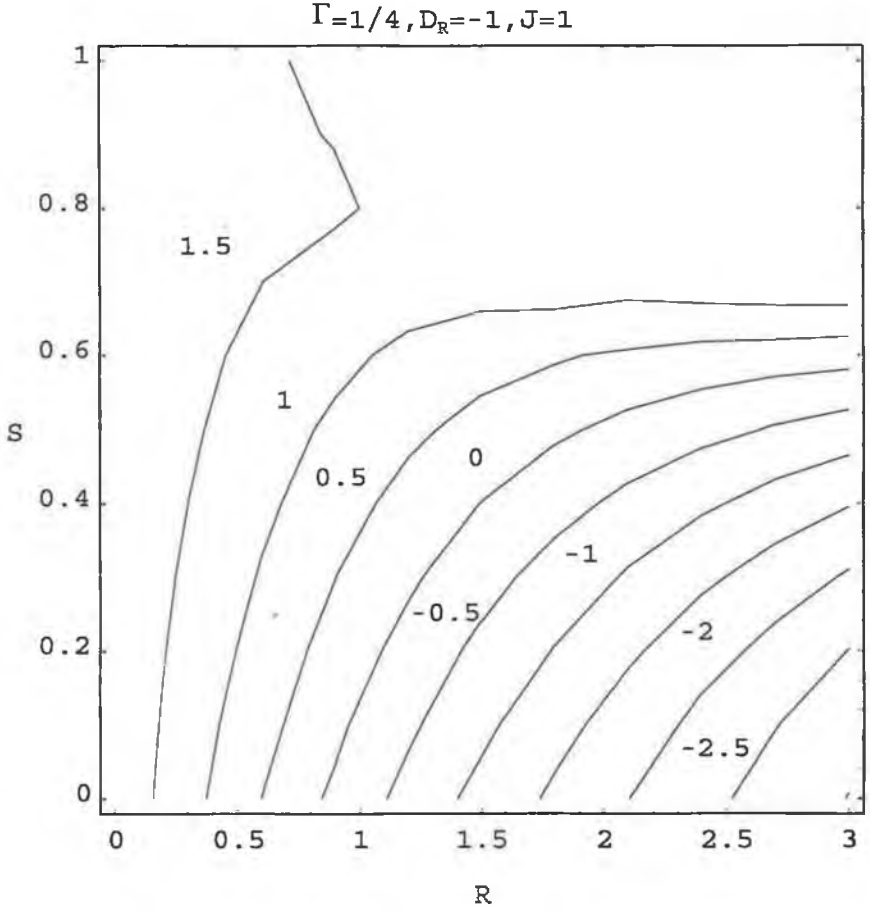

Figure 5-17: Contour Plot of Δ_0 for R[0,3] S[0,1] Γ=1/4, D_R=-1, J=1.

And again that interaction has more effect when viscosity is small.

Conclusion

We have shown that the resistive tearing mode in a cylindrical geometry can be studied by unsophisticated numerical methods, using modest computing resources. This is achieved by series of approximations and transformations. The linear stability of the tearing mode then depends on six parameters.

We can summarise our results in two main points. Firstly we can confirm that the destabilising change in the effective pressure gradient as flow increases, as described by Bondesson, Iacono and Bhattacharjee (1987), is valid in the tearing ordering. We also show that the destabilising interaction between flow and current, as first described by Paris and Sy (1983) in slab geometry, is also present in cylindrical geometry. The size of both these effects depends on the magnetic shear parameter, S, (as defined in (1.7)). This is interesting because in the absence of flow this parameter has little effect on stability.

Appendix

In this appendix is a more complete description of how the tearing mode equations are derived from the full MHD system. It is essentially a transcription of a set of notes I received from Dr. R.B. Paris.

Equilibrium:

Working in cylindrical co-ordinates, we consider an equilibrium of the form

$$\begin{aligned} \underline{B}_0 &= \{0, B_{0\theta}(r), B_{0z}(r)\} \\ \underline{V}_0 &= \{0, V_{0\theta}(r), V_{0z}(r)\} \\ p_0 &= p_0(r) \\ \rho_0 &= p_0(r) \end{aligned} \qquad \text{(A.1)}$$

which satisfy the divergence and incompressibility conditions

$$\begin{aligned} \nabla \cdot \underline{B}_0 &= 0 \\ \nabla \cdot \underline{V}_0 &= 0 \end{aligned} \qquad \text{(A.2)}$$

and hydrostatic balance.

$$p_0' = -(\nabla \times \underline{B}_0) \times \underline{B}_0 = -(B_{0\theta} D_* B_{0\theta} + B_{0z} D B_{0z}) \qquad \text{(A.3)}$$

$$\text{where} \quad D = \frac{d}{dr}, \quad D_* = \frac{d}{dr} + \frac{1}{r}. \qquad \text{(A.4)}$$

$$\text{Let} \quad b_\theta = \frac{B_{0\theta}}{B_0} \quad b_z = \frac{B_{0z}}{B_0}. \qquad \text{(A.5)}$$

We construct an orthonormal basis by defining unit vectors:

$$\underline{e}_r = \{1,0,0\} \quad \underline{e}_\parallel = \{0, b_\theta, b_z\} \quad \underline{e}_\perp = \underline{e}_r \times \underline{b} = \{0, -b_z, b_\theta \quad . \qquad \text{(A.6)}$$

The equilibrium current is given by:

$$\begin{aligned} J_0 &= \nabla \times \underline{B}_0 \\ \underline{e}_r \cdot \underline{J}_0 &= 0 \\ \underline{e}_{\parallel} \cdot \underline{J}_0 &= -b_\theta B_{0z}{}' + \tfrac{b_z}{r}\tfrac{\partial}{\partial r}(rB_{0\theta}) = b_z D_* B_{0\theta} - b_\theta D B_{0z} \end{aligned} \qquad (A.7)$$

while the velocity field in the new basis is given by:

$$\begin{aligned} v_{\parallel} &= b_\theta v_0 + b_z v_z \quad \left(v_z = b_\theta v_{\parallel} - b_z v_{\perp}\right) \\ v_{\perp} &= b_\theta v_z - b_z v_0 \quad \left(v_\theta = b_z v_{\parallel} + b_\theta v_{\perp}\right) \end{aligned} \qquad (A.8)$$

Because of the form of the equilibrium studied, perturbed quantities must vary like

$$f(r)\exp(im\theta + ikz + \omega t). \qquad (A.9)$$

For convenience we define some new parameters.

$$\text{Let } F = \tfrac{m}{r}B_{0\theta} + kB_z \quad G = \tfrac{m}{r}V_{00} + kV_z \quad H = kB_{00} - \tfrac{m}{r}B_z \qquad (A.10)$$

$$\text{and } K^2 = k^2 + \tfrac{m^2}{r^2}.$$

$$\text{Then} \quad \underline{e}_{\parallel} \cdot \nabla f = i\tfrac{F}{B_0} f \qquad \underline{e}_{\perp} \cdot \nabla f = i\tfrac{H}{B_0} f\ , \qquad (A.11)$$

where f is any smooth function of r.

Now we work on each equation separately

Divergence condition

$$\nabla \cdot \underline{B}_1 = 0 \quad \Rightarrow \quad D_* B_{1r} + i\tfrac{F}{B_0} B_{\parallel} + i\tfrac{H}{B_0} B_{\perp} = 0 \qquad (A.12)$$

Continuity Equation

$$\tfrac{\partial \rho}{\partial t} + \nabla \cdot \rho \underline{v} = 0 \quad \Rightarrow \quad \omega \rho_1 + v_{1r}\rho_0{}' + iG\rho_1 = 0 \qquad (A.13)$$

Induction Equation

$$\frac{\partial \underline{B}}{\partial t} = \nabla \times (\underline{v} \times \underline{B}) + \eta \nabla^2 \underline{B}$$

$$\Rightarrow \omega \underline{B} = \nabla \times (\underline{V}_0 \times \underline{B}_1) + \nabla \times (\underline{v}_1 \times \underline{B}_0) + \eta \nabla^2 \underline{B}_1 . \qquad \text{(A.14)}$$

Now $\nabla \times (\underline{V}_0 \times \underline{B}_1) = \underline{B}_1 \cdot \nabla \underline{V}_0 - \underline{V}_0 \cdot \nabla \underline{B}_1 \qquad \nabla \times (\underline{v}_1 \times \underline{B}_0) = \underline{B}_0 \cdot \nabla \underline{v}_1 - \underline{v}_1 \cdot \nabla \underline{B}_0$

Thus $\underline{e}_r \cdot \nabla \times (\underline{v}_1 \times \underline{B}_0) = iFv_{1r}$

$$\underline{e}_\parallel \cdot \nabla \times (\underline{v}_1 \times \underline{B}_0) = iFv_\parallel - \left(J_\perp - \frac{2B_{0\theta}^2}{rB_0} \right) v_{1r}$$

$$\underline{e}_r \cdot \nabla \times (\underline{V}_0 \times \underline{B}_1) = -iGB_{1r} \qquad \text{(A.15)}$$

$$\underline{e}_\parallel \cdot \nabla \times (\underline{V}_0 \times \underline{B}_1) = B_{1r} \left(D_- V_\parallel - \left(b_\theta{}' V_{0\theta} + \frac{b_z V_{0z}}{r} \right) \right) - iGB_\parallel \quad \text{where } D_- = \tfrac{d}{dr} - \tfrac{1}{r}.$$

The r - component of the induction equation is then

$$\omega B_{1r} = iFv_{1r} - iGB_{1r} + \eta \left(\left(DD_* - k^2 \right) B_{1r} - 2i \tfrac{m}{r^2} \left(b_\theta B_\parallel - b_z B_\perp \right) \right) \qquad \text{(A.16)}$$

and the || component is

$$\omega B_\parallel = iFv_\parallel - \left(J_\perp - \frac{2B_{0\theta}^2}{rB_0} \right) v_{1r} + B_{1r} \left(D_- V_\parallel - \left(b_\theta{}' V_{0\theta} + \frac{b_z V_{0z}}{r} \right) \right) - iGB_\parallel$$

$$+\eta \left(\begin{array}{l} \left(DD_* - k^2 \right) B_\parallel + \left(b_\theta b_\theta{}'' + b_z b_z{}'' + \frac{b_z^2}{r^2} \right) B_\parallel - 2 \left(b_\theta b_z{}' - b_z b_\theta{}' \right) \frac{\partial B_\perp}{\partial r} \\ + \left(b_z D_* D b_\theta - b_\theta D D_* b_z \right) B_\perp + 2i \frac{m}{r} b_\theta B_{1r} \end{array} \right). \qquad \text{(A.17)}$$

Momentum equation

$$\rho \left(\frac{\partial \underline{v}}{\partial t} + \underline{v} \cdot \nabla \underline{v} \right) + \nabla P = \underline{B} \cdot \nabla \underline{B} + \mu \nabla^2 \underline{v}$$

where $P = p + \frac{1}{2} B^2 \equiv$ kinetic and pressure terms

$$\Rightarrow \rho_0 (\omega \underline{v}_1 + \underline{V}_0 \cdot \nabla \underline{v}_1 + \underline{v}_1 \cdot \nabla \underline{V}_0) + \rho_1 (\underline{V}_0 \cdot \nabla \underline{V}_0) + \nabla P_1 = \underline{B}_0 \cdot \nabla \underline{B}_1 + \underline{B}_1 \cdot \nabla \underline{B}_0$$

where $\underline{V}_0 \cdot \nabla \underline{V}_0 = \left(-\frac{V_{0\theta}^2}{r}, 0, 0 \right)$ the centrifugal acceleration (A.18)

Magnetic terms

$$\begin{aligned}
&\underline{e}_r\text{component} = iFB_{1r} - 2\frac{B_{10}B_{0\theta}}{r}\\
&\underline{e}_\parallel\text{component} = iFB_\parallel + J_\perp B_{1r}\\
&\underline{e}_\perp\text{component} = iFB_\perp - J_\parallel B_{1r}
\end{aligned} \qquad \text{(A.19)}$$

Inertial and pressure terms:

$$\begin{aligned}
&\underline{e}_r\text{component} = \rho_0\left((\omega + iG)v_{1r} - 2\frac{v_{10}V_{0\theta}}{r}\right) - \rho_1\frac{V_{0\theta}^2}{r} + P_1'\\
&\underline{e}_\parallel\text{component} = \rho_0\left((\omega + iG)v_\parallel + v_{1r}\left(V_\parallel' - \left(b_\theta' V_{0\theta} + b_z' V_{0z}\right) + b_0\frac{V_{0\theta}}{r}\right)\right) + i\frac{F}{B_0}P_1\\
&\underline{e}_\perp\text{component} = \rho_0\left((\omega + iG)v_\perp + v_{1r}\left(V_\perp' - \left(b_0' V_{0z} + b_z' V_{0\theta}\right) + b_z\frac{V_{0\theta}}{r}\right)\right) + i\frac{H}{B_0}P_1
\end{aligned}$$

(A.20)

Viscous terms:

$$\begin{aligned}
&\underline{e}_r\text{component} = \mu_\perp\left(\left(DD_* - K^2\right)v_{1r} - 2i\tfrac{m}{r^2}\left(b_\theta v_\parallel - b_z v_\perp\right)\right)\\
&\underline{e}_\parallel\text{component} = \mu_\perp\left(\begin{array}{l}\left(DD_* - K^2\right)v_\parallel + \left(b_0 b_\theta'' + b_z b_z'' - \frac{b_z^2}{r^2}\right)v_\parallel + 2\left(b_z b_\theta' - b_\theta b_z'\right)\frac{\partial v_\perp}{\partial r}\\ +\left(b_z DD_* b_\theta - b_\theta DD_* b_z\right)v_\perp + 2\frac{b_\theta}{r^2}\frac{\partial v_{1r}}{\partial\theta}\end{array}\right)\\
&\underline{e}_\perp\text{component} = \mu_\perp\left(\begin{array}{l}\left(DD_* - K^2\right)v_\perp + \left(b_0 b_0'' + b_z b_z''\right)v_\perp - 2\left(b_z b_\theta' - b_\theta b_z'\right)\frac{\partial v_\parallel}{\partial r}\\ -\left(b_z DD_* b_\theta - b_\theta DD_* b_z\right)v_\parallel - 2\frac{b_z}{r^2}\frac{\partial v_{1r}}{\partial r} + \frac{b_\theta}{r^2}\left(b_z v_\parallel + b_\theta v_\perp\right)\end{array}\right)
\end{aligned}$$

(A.21)

Now we eliminate the pressure term from the r-component of the momentum equation using the operator

$$\underline{e}_r \cdot K^2 \nabla K^{-2} \nabla^* \underline{A} + K^2 A_r \qquad \text{where} \quad \nabla^* \underline{A} = \nabla \underline{A} - \underline{e}_r D_* \underline{A} = i\frac{F}{B_0} A_\parallel + i\frac{H}{B_0} A_\perp$$

$$= K^2 D K^{-2} \left(i\frac{F}{B_0} A_\parallel + i\frac{H}{B_0} A_\perp \right) + K^2 A_r \ .$$

(A.22)

After application of this operator the equation becomes

$$\rho_0 \left(D((\omega + iG) D_* v_{1r}) - D\left(v_{1r} \left(\tfrac{im}{r} D_* V_{0\theta} + ikV_{0z}' \right) \right) - K^2 (\omega + iG) v_{1r} \right) +$$

$$2K^2 \frac{v_{1\theta} V_{0\theta}}{r} - K^2 \rho_1 \frac{V_{0\theta}^2}{r} = -iF\left(DD_* - K^2\right) B_{1r} + 2\tfrac{im}{r^2} B_{0\theta} D_* B_{1r} -$$

$$2K^2 \frac{B_{0\theta} B_{1\theta}}{r} + iAB_{1r} + \mu_\perp \left(DD_* - K^2\right) \nabla^2 v_{1r}$$

$$\text{where} \quad A = F'' - \frac{F'}{r} + 2m\frac{B_{0\theta}'}{r^2} - \frac{6m}{r^3} B_{0\theta} \ .$$

(A.23)

Using (A.16) we rewrite the equation as

$$\rho_0 \left(D((\omega + iG) D_* v_{1r}) - D\left(v_{1r} \left(\tfrac{im}{r} D_* V_{0\theta} + ikV_{0z}' \right) \right) - K^2 (\omega + iG) v_{1r} \right) +$$

$$2K^2 \frac{v_{1\theta} V_{0\theta}}{r} - K^2 \rho_1 \frac{V_{0\theta}^2}{r} = \frac{iF}{\eta} \left(\omega B_{1r} - iFv_{1r} + iGB_{1r} \right) + 2\frac{kH}{r} \left(b_\theta + b_z \frac{F}{H} \right) B_\parallel -$$

$$2i\frac{F}{r} D_* B_{1r} - iAB_{1r} + \mu_\perp \left(DD_* - K^2\right) \nabla^2 v_{1r} \ .$$

(A.24)

The Tearing Ordering.

To make further progress, we have to order the various terms in the equations to simplify them. This implies making estimates for the relative sizes of the quantities involved and using this information to eliminate insignificant terms in each equation. We are interested in the case $\eta \to 0$. The ordering of the variables will be based on the small parameter ε which will be proportional to a positive power of η. We use what is known as the weak viscous tearing ordering. In this ordering flow is chosen to scale like $V_0 \sim \eta^{1/5}$. This allows us to neglect the effect of Alfven waves,centrifugal forces and the Kelvin-Helmholtz instability.

$$\eta \sim \varepsilon^5 \qquad \mu_\perp \sim \varepsilon^2 \qquad r - r_s \sim \varepsilon^2 \qquad \frac{\partial}{\partial r} \sim \varepsilon^{-2} \text{(perturbed quatities only)}$$

$$m, k \sim \varepsilon^0 \qquad v_\parallel, v_\perp \sim \varepsilon^3 \Rightarrow v_{1r} \sim \varepsilon^5$$

$$B_\parallel, B_\perp \sim \varepsilon^4 \Rightarrow B_{1r} \sim \varepsilon^4 B_{1r}^{(0)} + \varepsilon^6 B_{1r}^{(1)} \text{with } B_{1r}^{(0)'} = 0$$

$$\omega \sim \varepsilon^3 \qquad -\frac{2k^2 p_0'}{r_s (F')^2} \sim \varepsilon \qquad J_\perp \sim \varepsilon \qquad A \sim 1 \qquad \rho_0' \sim \varepsilon$$

$$F \sim F'(r - r_s) \sim \varepsilon^2 \qquad G \sim G'(r - r_s) \sim \varepsilon^3$$

(A.25)

We adopt the convention of displaying below each term the ε order of that term.

The induction equation in the r-direction (A.16) is

$$\begin{array}{cccccc} \omega B_{1r} = & iFv_{1r} & -iGB_{1r} & +\eta\left(\begin{pmatrix} DD_* & -K^2 \\ \varepsilon^{-4} & 1 \end{pmatrix} B_{1r}\right. & -2i\frac{m}{r^2}\left(b_\theta B_\parallel - b_z B_\perp\right)\Big) \\ \varepsilon^3.\varepsilon^4 & \varepsilon^2.\varepsilon^5 & \varepsilon^3.\varepsilon^4 & \varepsilon^5 \quad \varepsilon^4 & \varepsilon^4 \end{array}$$

Collecting terms of order ε^5 we get

$$B_{1r}^{(0)''} = 0 \qquad \text{so we consider the next order of } B_{1r}. \qquad \text{(A.26)}$$

Collecting terms of order ε^7

$$\eta B_{1r}^{(1)''} = (\omega + iG) B_{1r}^{(0)} + iFv_{1r}. \qquad \text{(A.27)}$$

Next we consider the parallel-component of the induction equation (A.17).

$$\underset{\varepsilon^7}{\omega B_\parallel} = \underset{\varepsilon^5}{iFv_\parallel} - \left(\underset{\varepsilon^2}{J_\perp} - \underset{\varepsilon^0}{\frac{2B_{0\theta}^2}{rB_0}}\right)\underset{\varepsilon^5}{v_{1r}} + \underset{\varepsilon^4}{B_{1r}}\left(\underset{\varepsilon^4}{D_- V_\parallel} - \underset{\varepsilon^4}{\left(b_\theta{}' V_{00} + \frac{b_z V_{0z}}{r}\right)}\right) - \underset{\varepsilon^7}{iGB_\parallel}$$

$$+\underset{\varepsilon^5}{\eta}\left(\begin{array}{l}\underset{\varepsilon^4}{\left(\underset{\varepsilon^{-4}}{DD_*} - \underset{\varepsilon^0}{K^2}\right)B_\parallel} + \underset{\varepsilon^4}{\left(b_\theta b_\theta'' + b_z b_z'' + \frac{b_z^2}{r^2}\right)B_\parallel} - 2\underset{\varepsilon^2}{\left(b_\theta b_z' - b_z b_\theta'\right)\frac{\partial B_\perp}{\partial r}} \\ \\ \underset{\varepsilon^4}{+\left(b_z D_* D b_\theta - b_\theta D D_* b_z\right)B_\perp} + \underset{\varepsilon^4}{2i\frac{m}{r}b_\theta B_{1r}}\end{array}\right).$$

We take terms of order ε^5

$$0 = iFv_\parallel + \frac{2B_{0\theta}^2}{rB_0}v_{1r} + \eta B_\parallel'' . \qquad \text{(A.28)}$$

Next we have the parallel part of the momentum equation

$$\rho_0\left(\underset{\varepsilon^3}{(\omega + iG)v_\parallel} + \underset{\varepsilon^3}{v_{1r}}\underset{\varepsilon^5}{\left(V_\parallel{}' - \underset{\varepsilon^3}{\left(b_\theta{}' V_{00} + b_z{}' V_{0z}\right)} + b_\theta\frac{V_{0\theta}}{r}\right)}\right) + i\underset{\varepsilon^6}{\frac{F}{B_0}P_1} = \underset{\varepsilon^6}{iFB_\parallel} + \underset{\varepsilon^2}{J_\perp}\underset{\varepsilon^4}{B_{1r}^{(0)}}$$

$$+\underset{\varepsilon^7}{\mu_\perp}\left(\begin{array}{l}\underset{\varepsilon^3}{\left(\underset{\varepsilon^{-4}}{DD_*} - \underset{\varepsilon^0}{K^2}\right)v_\parallel} + \underset{\varepsilon^3}{\left(b_0 b_\theta'' + b_z b_z'' - \frac{b_z^2}{r^2}\right)v_\parallel} + 2\underset{\varepsilon^1}{\left(b_z b_\theta' - b_0 b_z'\right)\frac{\partial v_\perp}{\partial r}} \\ \\ \underset{\varepsilon^3}{+\left(b_z D D_* b_\theta - b_\theta D D_* b_z\right)v_\perp} + \underset{\varepsilon^5}{2\frac{b_\theta}{r^2}\frac{\partial v_{1r}}{\partial\theta}}\end{array}\right).$$

We take terms of order ε^6

$$(\omega + iG)v_\parallel + i\frac{F}{B_0}P_1 = iFB_\parallel + J_\perp B_{1r}^{(0)} + \mu_\perp v_\parallel'' . \qquad \text{(A.29)}$$

Next we consider (A.24).

$$\rho_0\Bigg(\underset{\varepsilon^4}{D((\omega+iG)D_*v_{1r})}-\underset{\varepsilon^6}{D\left(v_{1r}\left(\tfrac{im}{r}D_*V_{0\theta}+ikV_{0z}\right)'\right)}-\underset{\varepsilon^8}{K^2(\omega+iG)v_{1r}}\Bigg)$$

$$+\underset{\varepsilon^6}{2K^2\frac{v_{1\theta}V_{0\theta}}{r}}-\underset{\varepsilon^{10}}{K^2\rho_1\frac{V_{0\theta}^2}{r}}=\underset{\varepsilon^{-3}}{\frac{iF}{\eta}}\left(\underset{\varepsilon^7}{\omega B_{1r}}-\underset{\varepsilon^7}{iFv_{1r}}+\underset{\varepsilon^7}{iGB_{1r}}\right)+\underset{\varepsilon^4}{2\frac{kH}{r}\left(\underset{\varepsilon^0}{b_\theta}+\underset{\varepsilon^2}{b_z\frac{F}{H}}\right)B_\parallel}\,We$$

$$-\underset{\varepsilon^6}{2i\frac{F}{r}D_*B_{1r}^{(1)}}-\underset{\varepsilon^4}{iAB_{1r}}+\underset{\varepsilon^7}{\mu_\perp}\left(\underset{\varepsilon^{-4}}{DD_*}-\underset{\varepsilon^0}{K^2}\right)\underset{\varepsilon^{-4}}{\nabla^2}\,\underset{\varepsilon^5}{v_{1r}}$$

take terms of order ε^4

$$(\omega+iG)v_{1r}''=\frac{iF}{\eta}\left(\omega B_{1r}^{(0)}-iFv_{1r}+iGB_{1r}^{(0)}\right)+2\frac{kHb_\theta}{r}B_\parallel-iAB_{1r}^{(0)}+\mu_\perp v_{1r}^{IV}.$$

(A.30)

Next we have the perpendicular component of the momentum equation

$$\rho_0\Bigg(\underset{\varepsilon^3}{(\omega+iG)v_\perp}+\underset{\varepsilon^3}{v_{1r}}\underset{\varepsilon^5}{\left(V_\perp'-\left(b_\theta'V_{0z}+b_z'V_{0\theta}\right)+b_z\frac{V_{0\theta}}{r}\right)}\Bigg)+\underset{\varepsilon^4}{i\frac{H}{B_0}P_1}=\underset{\varepsilon^6}{iFB_\perp}+\underset{\varepsilon^0}{J_\parallel}\,\underset{\varepsilon^4}{B_{1r}^{(0)}}$$

$$+\underset{\varepsilon^7}{\mu_\perp}\Bigg(\begin{array}{l}\underset{\varepsilon^3}{\left(\underset{\varepsilon^{-4}}{DD_*}-\underset{\varepsilon^0}{K^2}\right)v_\perp}+\underset{\varepsilon^3}{\left(b_\theta b_\theta''+b_zb_z''\right)v_\perp}+\underset{\varepsilon^1}{2\left(b_zb_\theta'-b_\theta b_z'\right)\frac{\partial v_\parallel}{\partial r}}\\ \underset{\varepsilon^3}{+\left(b_zDD_*b_\theta-b_\theta DD_*b_z\right)v_\parallel}+\underset{\varepsilon^3}{2\frac{b_z}{r^2}\frac{\partial v_{1r}}{\partial r}}+\underset{\varepsilon^3}{\frac{b_\theta}{r^2}\left(b_zv_\parallel+b_\theta v_\perp\right)}\end{array}\Bigg).$$

We collect terms of order ε^4

$$i\frac{H}{B_0}P_1=J_\parallel B_{1r}^{(0)} \qquad (A.31)$$

Combining with the parallel component of the momentum equation (A.29).

$$(\omega+iG)v_\parallel=iFB_\parallel+\left(J_\perp+\frac{F}{H}J_\parallel\right)B_{1r}^{(0)}+\mu_\perp v_\parallel'' \qquad (A.32)$$

Collecting the equations(A.26,A.27,A.30,A.28,A.32) together we get the system

$$B_{1r}^{(0)''} = 0$$

$$\eta B_{1r}^{(1)''} = (\omega + iG)B_{1r}^{(0)} + iFv_{1r}$$

$$(\omega + iG)v_{1r}'' = \frac{iF}{\eta}\left(\omega B_{1r}^{(0)} - iFv_{1r} + iGB_{1r}^{(0)}\right) + 2\frac{kHb_\theta}{r}B_\parallel - iAB_{1r}^{(0)} + \mu_\perp v_{1r}^{IV}$$

$$0 = iFv_\parallel + \frac{2B_{0\theta}^2}{rB_0}v_{1r} + \eta B_\parallel''$$

$$(\omega + iG)v_\parallel = iFB_\parallel + \left(J_\perp + \frac{F}{H}J_\parallel\right)B_{1r}^{(0)} + \mu_\perp v_\parallel''$$

(A.33)

Renaming variables and parameters gives us the system (1.9) in the text.

References

B. Coppi, J.M. Greene and J.L. Johnson (1966) "Resistive Instabilities in a Diffuse Linear Pinch" *Nuclear Fusion*, Vol.6 pp101-117.

R.B. Paris and W. N-C. Sy (1983) "The influence of Equilibrium Shear Flow along the Magnetic Field on the resistive tearing instability" *The Physics of Fluids*, Vol.26 No.10 pp2966-2975.

R.B. Paris (1982) "Lectures on Resistive Instabilities in MHD" *Euratom-CEA report*.

A. Bondesson, R. Iacono and A. Bhattacharjee (1987) "Local Magnetohdrodynamic instabilities of cylindrical plasma with sheared equilibrium flows" *The Physics of Fluids*, Vol.30 No.10 pp2966-2975.

L.Hou (1994) "The Effects of Flow on Resistive Instabilities in Magnetohydrodynamics" Ph.D. thesis University of Abertay Dundee.

R.Y. Dagazian and R.B. Paris (1986) "Stationary states of dissipative modes in cylindrical geometry" *The Physics of Fluids*, pp762-768.

A.Bondesson and M.Persson (1986) "Resistive tearing modes in the presence of equilibrium flows" *The Physics of Fluids*, Vol.29 No.9 pp2997-3007.

H.P.Furth,J.Killeen and M.N.Rosenbluth (1963) "Finite Resistive Instabilities of a Sheet Pinch" *The Physics of Fluids* Vol.6 No.4. pp459-484.

J.L. Johnson, J.M. Greene and B. Coppi (1963) "Effects of Resistivity on Hydromagnetic Instabilities in a Multipolar System" *The Physics of Fluids*, Vol.6 No.8 pp1169-1183.

D.Biskamp (1993) "Non-linear Magnetohydrodynamics" Cambridge University Press.

L.Hou, R.B.Paris and A.D. Wood (1996) "The resistive interchange mode in the presence of equilibrium flow" *The Physics of Plasmas* Vol.3 No.2 pp473-481.

R.B. Paris, A.D. Wood and S.Stewart(1993) "Effects of equilibrium flow on the resistive tearing mode" *The Physics of Fluids B* Vol.5 No.3.

R.B. Paris and A.D. Wood (1993) "The effects of flow on resistive instabilities in MHD" *Technical Report to Euratom.*